Анотація

Дипломний проект освітньо кваліфікаційного рівня «магістр» за спеціальністю 131 Прикладна механіка, спеціалізації «Динаміка і міцність машин та опір матеріалів» на тему: «Проектування високонавантаженого однозрізного з’єднання метал - композит мінімальної маси».

Проект складається з вступу, п’яти розділів, висновків і списку використаних джерел. Робота містить 74 сторінку, 29 таблиць, 39 рисунків

Актуальність роботи полягає в тому, що конструкції з типом з'єднань композит – композит і композит – алюміній досліджені тільки для стандартних схем армування (0, ±45, 90) градусів, натомість намотування виробів з використанням вуглепластику у вигляді джгутів, стрічок і в перспективі вуглетканини широко використовується під час розробки нових дизайнів фюзеляжів, оперення літаків, ракет, при цьому пакет композиційного матеріалу має в своєму складі шари армування (0, ±15, ±30, ±45, ±60, ±75, 90) що і підлягає дослідженню в моїй роботі.

Мета роботи – дослідити роботу з'єднань метал – композит, при армуванні шарів композиту (0, ±15, ±30, ±45, ±60, ±75, 90) градусів відповідно.

Завдання роботи:

- Визначити матриці жорсткості для пакету монослоїв
- Дослідити вплив різних параметрів (діаметр болтів, пружні характеристики, товщина пакету) на розподілення навантаження між елементами кріплення.
- Оптимізація однозрізного з’єднання метал – композит для рівномірного розподілення зусиль в елементах кріплення

Розрахунок виконаний за допомогою напівемпіричних методів. Всі розрахунки проводяться в Excel і NX Patran. Оскільки розрахунок проводиться за іноземними методиками, всі обчислення проводяться в американській системі одиниць.

Ключові слова: *композит, гнучкість елементів кріплення, жорсткість системи*

Abstract

The master`s degree dissertation of specialty 131 Mechanics, specialization “Dynamics and Strength of Machines and Strength of materials” on topic “Design of single shear metal-composite joint of minimum mass”

The dissertation consists of introduction, five parts, conclusions and references. The project contains 74 pages, 39 figures, 29 tables.

The urgency of the chosen topic is that the structures with the type of joints composite – composite and composite – aluminum are investigated only for standard schemes of reinforcement (0, ±45, 90) degrees, instead of winding products using carbon fiber in the form of bundles, tapes and in carbon perspective, it is widely used in the development of new aircraft or missile fuselage designs, with the composite package having reinforcement layers (0, ±15, ±30, ±45, ±60, ±75, 90 in its composition) which is the subject of research in my work.

The purpose of the work is to investigate the work of metal - composite joints, with the reinforcement of the composite layers 0, ±15, ±30, ±45, ±60, ±75, 90 degrees respectively.

Tasks of the work:

- Determination of the stiffness matrix for the monolayer package
- Investigation of the influence of various parameters (bolt diameter, package thickness elastic properties)
- Optimization single shear metal-composite joint

The design is done using semi-empirical methods. All calculations are carried out in Excel and NX Patran. Since the calculation is carried out according to a foreign method, all calculations are performed in the American measurement system.

Keywords: *composite, fastener flexibility, system rigidity*

Table of contents

Introduction

Background

Bolted joints are widely used when connecting structural components in larger configurations. Information about the load distribution and fastener flexibility among fasteners in a joint is of interest in the design of lightweight structures, commonly occurring in the field of aeronautics. Aircraft structures, in particular the fuselage and wings, are often connected using bolted joints with various types of fasteners. A sketch of a bolted joint is shown in Figure 1.

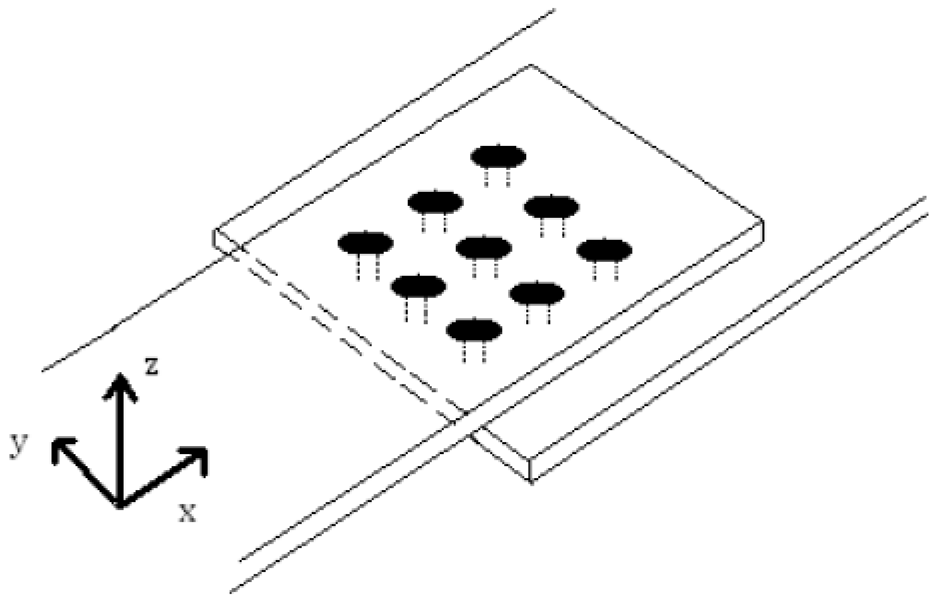

Figure 1 Example joint

The load distribution between the fasteners in the joint has a large impact on factors that affect the strength and fatigue life of the joint, such as bearing pressure and stress concentrations, and is therefore of interest when designing and sizing such a structure.

Fastener flexibility is a property of interest when calculating the load distribution in a joint. It is a measure of the fastener's influence on the flexibility of the joint, and has a large impact on load distribution, as illustrated in Figure 2.

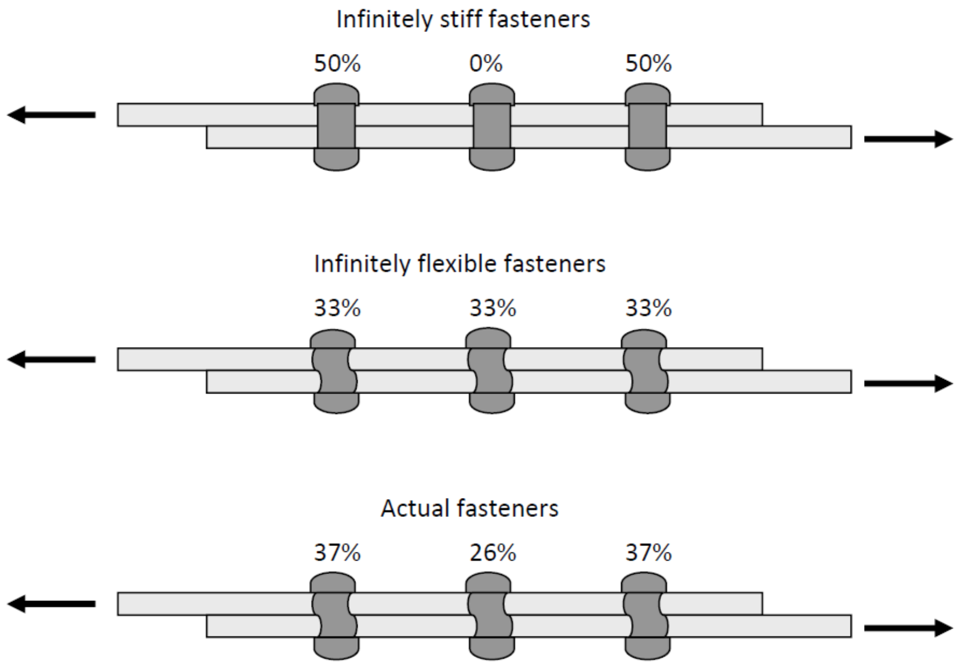

Figure 2 Cross-section of a joint; load distribution with varying fastener flexibility

Since the inception of technology, there were various problems associated with their development, implementation, operation, maintenance, utilization. Over time and technological progress, some achievements are being replaced by more ideal and effective ones. Nowadays, an important driving factor is the value for money, of course, taking into account other features that can be combined into a large group of technical and economic requirements. Efficiency is determined for each industry individually. Efficiency also depends on the nature of the item being evaluated. For materials in the field of mechanical engineering the value for money, cost and durability, durability and weight are relevant. This is due to the fact that reducing the weight of the structure allows you to save energy and therefore reduce the cost of operation. However, the weight reduction of the structure must occur without reducing the load capacity of the structure to maintain reliability and performance. Now the actual solution is to use composite materials with different properties that can be set in advance. [1]

A composite material is a material made from two or more constituent materials with significantly different physical or chemical properties that, when combined, produce a material with characteristics different from the individual components. The use of composite materials has its advantages and disadvantages depending on the type of material. Common to all the advantages is the high strength-to-weight ratio, high rigidity, and linearity of the stress-strain diagram up to failure.

Fittings are the main existence and functioning of everything on Earth, so there were no periods and there were no organizations, enterprises and individuals who wouldn`t solve the problem of connecting something with something. A properly designed and implemented fitting ensures success, and failure can even lead to disastrous consequences (for example wing to body structure joint). According to statistics, the compounds contribute up to 20% of their mass to the aircraft structure and are responsible for 80% of accidents and disasters. Aircraft structures are distinguished by a large number of functional, operational and technological connections and joints, which on the one hand are sources of irregularity of the stress-strain state, and on the other hand, they require some special properties of the material at the place of joint parts (hardness, wear resistance, tendency to self-healing microcracks etc.).[1]

1. Overview of existing metal-composite joints

In order to reduce the weight of aircraft structures, they tend to increase the efficiency of the materials used and existing technologies. Composite materials and parts based on them in the aerospace industry have been widely used in recent years due to their unique properties, such as low density, high strength, corrosion resistance, low thermal conductivity, high integration etc. It is not always possible to increase the efficiency and overall volume of CM in aircraft structures due to the high cost of these materials, and it`s also due to a number of problems associated with the difficulties of connecting parts of the CM with each other, as well as with the metal structure of the elements. All the advantages and disadvantages of CM are explained from the anisotropic structure, significant differences in properties in different directions, and the imperfection of design techniques for composite units. Calculation of physical and mechanical characteristics of materials also causes certain difficulties. [2]

Due to its polymer structure, CM adheres well or welds, as in the case of using a thermoplastic matrix. Adhesive and polymer matrix of any nature are very brittle materials with low strength characteristics and poor perception of shear stresses. The critical physical and mechanical characteristic of both adhesive and welded joints is the shear modulus. According to experimental data, the ultimate load in adhesive joints is about 8600 lb/in, which is not enough to transfer forces in aircraft structures. Therefore, mechanical types of joints are used. The holes for mechanical fasteners have always been considered a stress concentrator for a structure made of any material, as these are a source of cracks and defects that reduce the bearing capacity of the structure entirely. For fibrous plastics, this is a particularly acute problem, because in the construction of CM, the main supporting element is fiber. When the fiber is destroyed and the holes for mechanical fasteners are drilled in the parts made from CM, the load-bearing capacity of the structure drops sharply. Since mechanical connections of parts are made from CM, the strength is reduced by 2-4 times in comparison with a similar connection of metal parts. This leads to a significant increase mass of the structure, since it is necessary to increase the thickness of the parts included in the connection, which reduces the efficiency of using CM or necessitates the use of special structurally technological solutions (STS), taking into account the specifics of composites. Fragmentary foiling (Figure 3 (a)), gluing washers on both sides for mechanical fasteners (Figure 3 (d,e)), gluing bushings of different configurations(Figure 3 (b, c)), hole formation (by shearing fibers and dispersion strengthening of the resin in order to volumetric fiber content) all this increases the ultimate loads transmitted by the connections. [2]

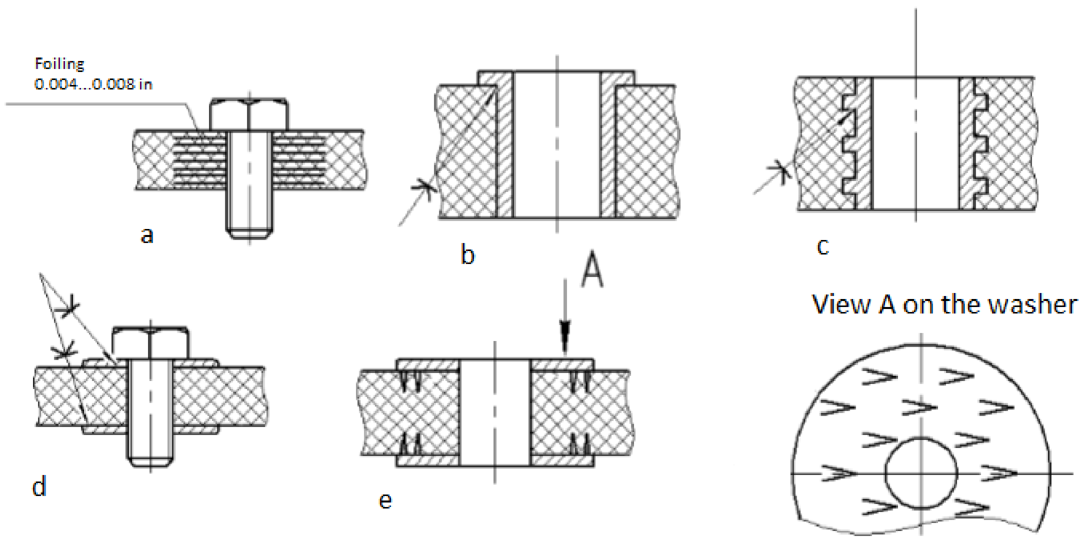

Figure 3 Some of the STS which increase load-bearing capacity

The problems of connecting parts from CM by themselves or by metal structural elements are solved through the use of integrated shaping of nodes and joints in composite details. They have proven themselves well and are quite actively used in compounds in joint elements. For example, to transfer longitudinal forces in the areas of the joints of parts, volumetric STS with longitudinal and transverse connections are used. [2]

1.1. Mechanical Joining

Mechanical fastening refers to the use of bolts and rivets to bond composites to other metals. Mechanical fasteners are mainly used for single lap joints (rivets and bolts), double lap joints (bolts), and for flanges (bolts). The high tensile strength and peel force of bolts and rivets, tolerance to thermal and high humidity environments, simplicity of use and ease of repair, make this joining technique most popular. However, damage to the reinforcing fibres and weakening of the cross-section through drilling, stress concentrations around the bearing holes and problems with fitting clearance, are major drawbacks for this technique, especially when applied to CFRP. In addition, the fasteners themselves and joint overlap are an important source of weight increase.[3]

1.2. Adhesive Joining

Adhesive joining involves the use of adhesives which hold materials together by surface attachment. Adhesives are normally epoxy resin based, but can be acrylic, phenolic, or polyurethane based. They come in liquid, paste or film form and cure at temperatures from room temperature to 170°C. Adhesively bonded joints have many advantages, such as light weight, a uniform stress distribution, design flexibility, simplicity of fabrication and the ability to bond structural components with different mechanical and thermal properties. Nevertheless, adhesive bonded joints cannot be disassembled without damage. Furthermore, these joints are very sensitive to environmental factors like humidity and temperature, in addition to other design parameters, such as bonding clearances, type and structure of adherend and surface roughness and can have low toughness and creep resistance. The most serious problem for adhesive bonding, however, is the uncertainty regarding the long-term structural integrity due to environmental degradation. This failure behaviour can result in the introduction of "safety-rivets", or an increased overlap of the joining partners, which again increases weight.[3]

1.3. Hybrid Joining and Hyper-Joints

The Hyper – Joints studied in this project were an innovative form of hybrid joints with the same intent of combining the benefits of mechanical joining with adhesive bonding. Like other hybrid joining processes, the goal with hyper-joints is the formation of an integral joint between the composite material and the metal component to form a composite structure having excellent load bearing capacity. Hyper-joints involve the use of arrays of small metal pins/protrusion which are manufactured on to the surface of the base metal. The metal pins/protrusions are then integrated with the composite laminate without breaking the fibres before curing the resin. This improves the joint strength both via the adhesion and mechanical fit through the thickness of the composite. The small size of the pins (not more than 0.12 in. but more typically ~ 0.04 in. in diameter) and the means of providing the mechanical joining clearly distinguish this novel approach from conventional hybrid joining process. The pins must be small in diameter to avoid damaging the composite on insertion. The small size and geometry of the pins thus limits the manufacturing routes that can be used.

Joints are perhaps the most common source of failure in aircraft structure and therefore it is most important that all aspects of joints design are given consideration during the structural design. Failures may occur for various reasons, such as secondary stresses due to eccentricities, stress concentrations excesive deflection, etc. , or some combination of conditions, all of which are difficult to evaluate to an exact degree. These factors directly affect the strength of joint, especially the fastened joints which are greatly weakened by notch effect. .[3]

1.4.Comparison of joining methods

Assembly joints, which occur when any two components are assembled, are a major source of stress concentrations. In the case of bonded joints, stress concentrations occur to maintain strain compatibility between bonding component. In the case of mechanical primary purpose of this section is to acquaint the engineer with some of the problem areas encountered, introduce some of the joint design allowables generated on the subject, and show a few examples of how typical problems have been solved.[4]

To fully realize the potential of advanced composites in lightweight aircraft structure, it is particularly important to ensure that the joints, either bonded or fastened, don`t impose a reduced efficiency on the structure. This problem is far more severe with composite materials than with conventional metals because the high-specific-strength composite filaments are relatively brittle. Composites have very little capacity to redistribute loads as shown in Figure 4 [4] and practically none of the forgiveness of a yielding metal to mask a multitude of design approximations. This is the reason why greater efforts are devoted to understanding joints in composite materials and to providing reliable design techniques, particularly for thicker sections and for multiple fastener pattern design cases. [4]

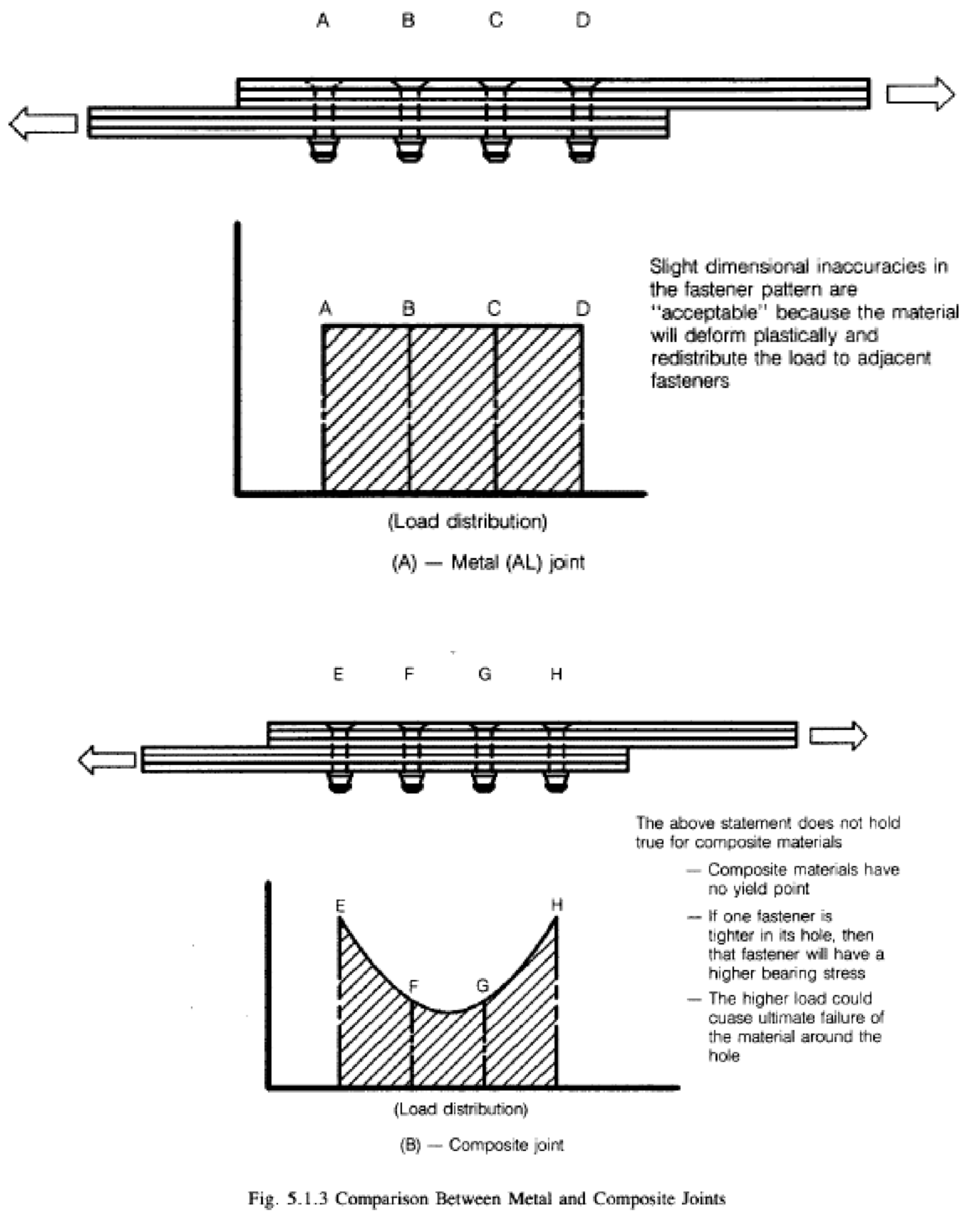

Figure 4 Comparing load distribution in metal and composite joint

Method		Anticipated Benefits	Limitations
Mechanical fastening		- Mature technology - Baseline for cost data - Could supplement weld/bond assembly methods	- Low risk - Increased weight - Labor intensive - Requires secondary seal - Shimming fit-up stress
Adhesive bonding		- Reduced fastener count/weight	- Moderate risk - Cure cycle required - Tooling
Thermoplastic welding	- Resistance	- Can be automated process - Continuous weld - Reduced fastener count/weight	- Moderate risk - Requires 2 side access
	- Ultrasonic	- Can be automated process - Possible continuous weld - Reduced fastener count/weight	- Moderate risk - Requires 2 side access
	- Induction	- Requires 1 side access - Can be automated process - Continuous weld - Reduced fastener count/weight	- Moderate – high risk - Requires magnetic susceptor material
Cocuring		- Total homogeneous weld joint - Probable elimination of seal	- Low risk - Part size/shape limited

Table 1 Comparison of joining methods

1.5. Calculation fastener flexibility

1.5.1. Defining fastener flexibility

The fastener flexibility concept was introduced by Tate & Rosenfelt in 1946 [5], under the alias "bolt constant", due to a desire to calculate load distribution in joints with multiple rows. It is defined by assuming a linear relationship between the displacement due to the presence of the fastener, and the load transfer. The fastener flexibility *f* can be written as

$$f = \frac{1}{k} = \frac{\delta}{P_{LT}}$$

where k is the fastener stiffness, P_{LT} the load transferred by the fastener (defined in Figure 5), and δ the contribution to the total displacement of the joint disregarding the elongation PL/EA of the plates. Thus, the fastener flexibility includes all phenomena that affect the flexibility of the joint (apart from plate flexibility) such as fastener deformation, fastener tilt, and deformation of fastener holes. In determining the fastener flexibility experimentally, there are several approaches, of which a few are described here.

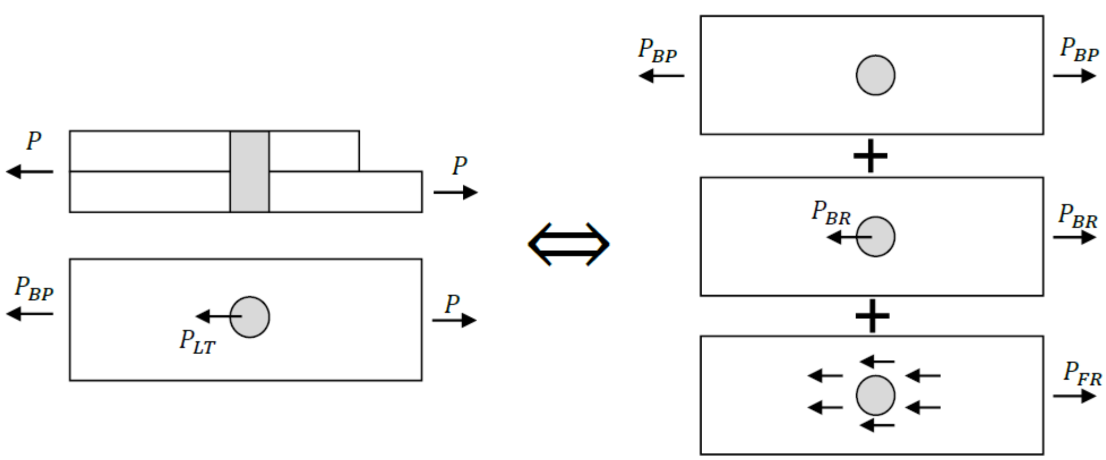

Figure 5 Forces acting on a joint: transferred load (P_{LT}), bypassing force (P_{BP}), bearing force (P_{BR}), frictional force (P_{FR})

Jarfall [6] measured the gap g of Figure 6 for the applied force 2P.

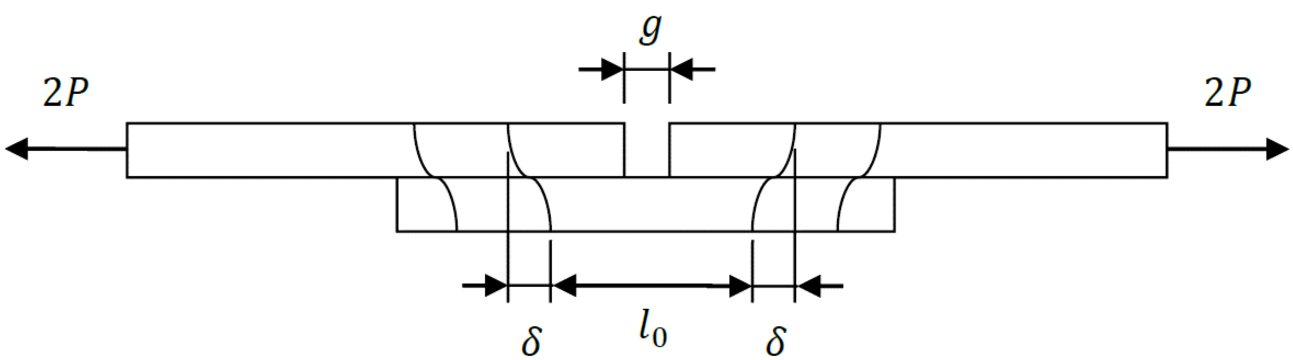

Figure 6 Finding fastener flexibility (Jarfall)

The gap g relates to δ as

$$\Delta g = \Delta l_0 + 2\delta$$

This yields

$$\frac{\partial g}{\partial P} = \frac{2l_0}{AE} + 2f$$

and the fastener flexibility becomes

$$f = \frac{1}{2}\frac{\partial g}{\partial P} - \frac{l_0}{AE}$$

Huth [7] performed measurements on the total displacement Δl_{tot} between points A and B of the single shear geometry with two fasteners in Figure 7 thus yielding average values of δ

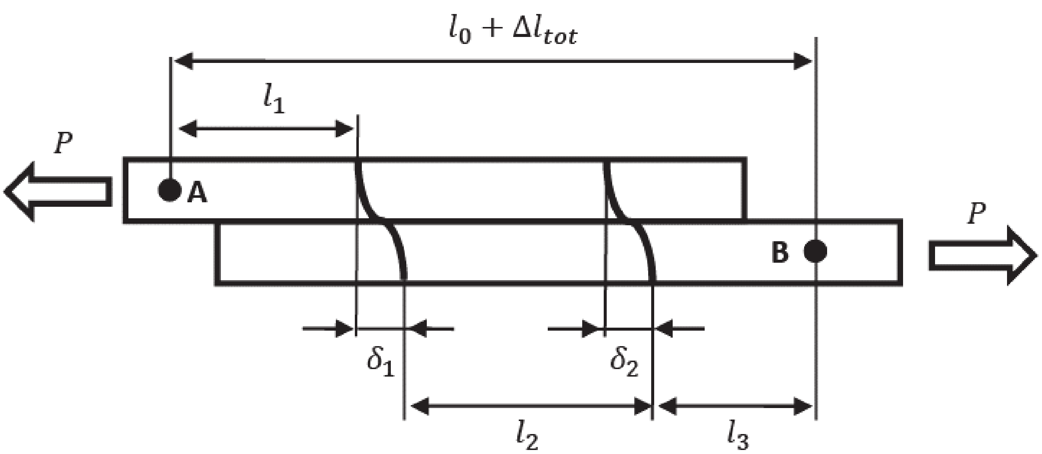

Figure 7 Finding fastener flexibility (Huth, single shear)

The total displacement is written as

$$\Delta l_{tot} = \frac{\delta_1 + \delta_2}{2} + \Delta l_1 + \Delta l_2 + \Delta l_3$$

From this δ becomes

$$\delta = \frac{\delta_1 + \delta_2}{2} = \Delta l_{tot} - \Delta l_{elast}$$

Where, with the plate width ω , thickness *t*, and Young`s modulus *E*,

$$\Delta l_{elast} = \frac{P}{t_1 \omega E_1}\left(l_1 + \frac{l_2}{\left(\frac{t_2}{t_1}\frac{E_2}{E_1}\right)} + \frac{l_3}{\left(1 + \frac{t_2}{t_1}\frac{E_2}{E_1}\right)} \right)$$

And the fastener flexibility is

$$f = \frac{1}{2}\frac{(\delta_1 + \delta_2)}{\frac{P}{2}} = \frac{\delta_1 + \delta_2}{P}$$

The relationship between force and displacement is in reality non-linear, and therefore there are several ways to identify a fastener flexibility (as a constant) from experimental data. Jarfall [6] describes some of these methods thoroughly. The way that is probably most representative when striving for an elastic model to describe the behavior of a joint, is the Jarfall alternative d, which was also used by Huth. Figure 8 shows a sketch of the characteristic behavior of a joint when subjected to cyclically increasing load, where also the fastener flexibility as obtained by Huth is indicated.[1]

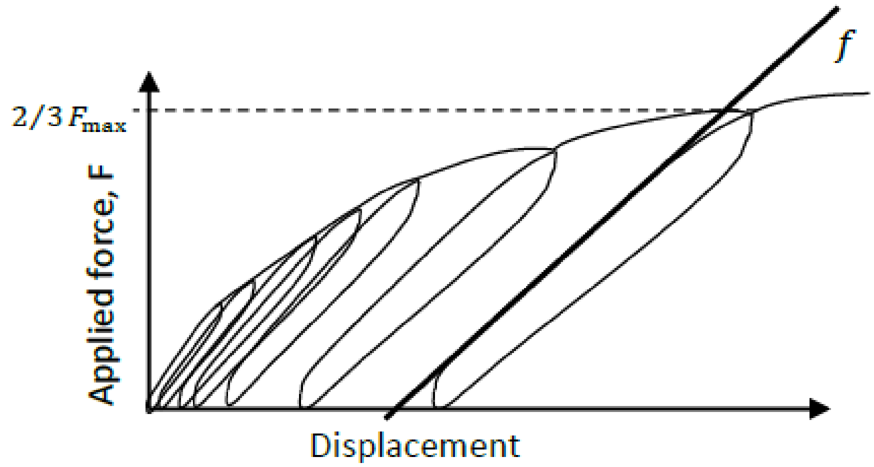

Figure 8 Example of measured fastener flexibility

1.5.2. Overview of methods

As seen, there are several ways to find the fastener flexibility experimentally. Many have attempted - via testing on geometries with varying parameters - to create methods for describing the joint behavior by calculating the fastener flexibility as a function of these parameters. These include empirical formulas derived from specific types of joints and materials by Grumman, Huth [7], Boeing, Douglas , Tate & Rosenfeld [5] and others, using an analytical approach such as methods by Barrois [8] and ESDU [9]. The great variety of available methods is due to the fact that they have been derived using different simplifications and/or that they apply to specific materials or specific types of joints.[1]

Things that affect the joint behavior include bolt pre-tension, fastener fit (hole clearance), hole surface quality, type of fastener (countersunk, rivets, bolts), surface quality including coatings or sealants and more.

Two common configurations occur when referring to joints and fastener flexibility, namely single shear and double shear loaded fasteners, illustrated in Figure 9

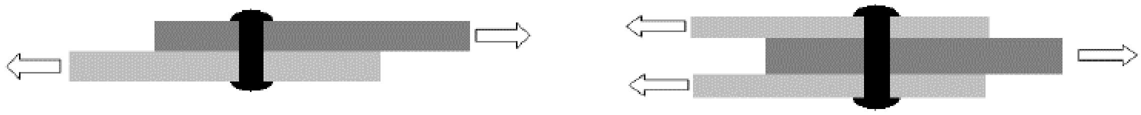

Figure 9 Types of shear

In the case of single shear, another physical phenomenon presents itself due to the fastener tilting under that kind of load, called secondary bending. Even with the external load being free from bending moment, the tilting of the fastener that occurs in single shear induces bending in the joint which has a high impact on fatigue life of joints.[1]

1.5.3. Grumman

The Grumman equation is an empirically derived formula that was presented by the Grumman Aerospace Corporation

$$f = \frac{(t_1 + t_2)^2}{E_f d} + 3.72 \cdot \left(\frac{1}{E_1 t_1} + \frac{1}{E_2 t_2}\right)$$

Where E_f and d are the Young`s modulus and diameter of the fastener, respectively.

The conditions under which the testing was performed, that eventually lead up to the Grumman formula, is unclear. Nordin [10] claims it was derived for metallic materials, for which both bolts and rivets can be used in joining plates. It was however used during the development of a composite component for the Viggen aircraft, which are usually not joined by rivets. The formula does however not account for fastener tightening, hole clearance, and whether the fastener is countersunk or not [10].

1.5.4. Huth

Based on extensive testing on different types of joints and materials, a formula for fastener flexibility was fitted to load-displacement curves as

$$f = \left(\frac{t_1 + t_2}{2d}\right)^a \frac{b}{n}\left(\frac{1}{E_1 t_1} + \frac{1}{nE_2 t_2} + \frac{1}{2E_f t_1} + \frac{1}{2nE_f t_2}\right)$$

Where a, b and n are parameters defining the joint type as seen in

Single shear	$n = 1$
Double shear	$n = 2$
Bolted metallic joints	$a = 2/3$, $b = 3.0$
Riveted metallic joints	$a = 2/5$, $b = 2.2$
Bolted graphite/epoxy joints	$a = 2/3$, $b = 4.2$

Table 2 Huth parameters

1.5.5. Barrois

The method by Barrois was developed using an analytical approach by modeling the fastener as a beam on an elastic foundation, taking into account bending and shearing deflections of the fastener. The assumption is made that there is a linear relation between the deflection of the fastener and the applied load. Also, it is assumed there is no clearance between fastener and foundation. Both single shear and double shear loaded fastener installations are handled.

In the derivation it is assumed that the joined plates are of the same material. Finally, two different boundary conditions are applied at the fastener ends, yielding several ways of using Barrois` method (`variants'). These boundary conditions are: clamped fastener heads (bolts) and free fastener heads (pins). Barrois uses a single-spring assumption, similar to Huth. Also, in calculating load distribution.

The Barrois derivation of the fastener flexibility is quite extensive and not reproduced in detail in this report. The interested reader may find a detailed description of the method by Barrois in Reference [8].

1.5.6. Tate

The analysis of load transfer through mechanically fastened joints in fibrous composite laminates must inevitably rely upon some empirically derived input based on test results. This is so because fiber reinforced resins do not fail as homogeneous one-phase materials, although they are usually modeled as such, but as heterogeneous materials with two distinct phases and an interface. As shown in Figure 10, the efficiency of real composite bolted joints lies roughly halfway between analytical predictions based on purely elastic and perfectly plastic behavior. Analysis based on either extreme does not come close to predicting the strength of these single-row bolted joints, and either extreme would not be acceptable for design purposes without some form of major modification. All analyses of composite bolted joints rely on an empirical correlation factor in some form or other.

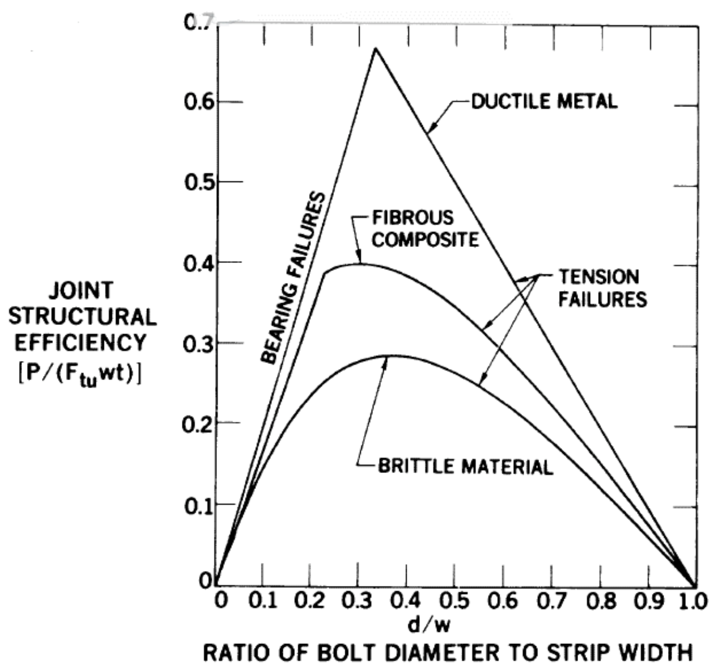

Figure 10 Relation between strengths of bolted joints in ductile, fibrous composite and brittle materials

All attempts to interpret the stiffness data for the single-shear tests in terms of existing formulas for metal joints failed. So the double-shear formula [5] was modified to account for the bolt rotation that occurs in single-shear joints. The first term, representing the shear deformation of the bolt, was taken to be unaltered. The second term, accounting for bolt bending, was deleted and the remaining three terms were all multiplied by the factor (1 + 3β), where β represents the fraction of the bending moment on the bolt that is reacted by the nonuniform bearing stresses across the thickness. This is explained in Figure 11. The remaining fraction (1 – β) is reacted by the head and nut on the bolt. Therefore, β would vary from a maximum value of 1.0 for a simple shear pin, through a value of about 0.5 for countersunk fasteners, to a small fraction for torqued bolts with protruding heads, becoming very small for the combination of large washers with a large diameter-to-thickness ratio. The interpretation of the data from these tests, with a d/t ratio of about 2 and relatively small washers, indicates that β is on the order of 0.15 here. The need for the correction factor β arises because, as the fasteners rotate under single-shear loading, the bearing stresses become more concentrated near the interface between the members than is the case with double-shear loading. Consequently, the relative motion is increased by those locally higher bearing stresses.[11]

$$\frac{1}{K} = \frac{\delta}{P} = \frac{2(t_1 + t_2)}{3G_b A_b} + \frac{2(t_1 + t_2)}{t_1 t_2 E_{b_{br}}} + \frac{1}{t_1(\sqrt{E_L E_T})_1} + \frac{1}{t_2(\sqrt{E_L E_T})_2} \cdot (1 + 3\delta)$$

The joint flexibility in single shear is thus expressed by the relation in which the subscripts 1 and 2 identify the two members. Figure 11 compares the stiffness predictions of this formula with the measured results. Had the β term not been included, the stiffness would have been overestimated by about 50 percent.

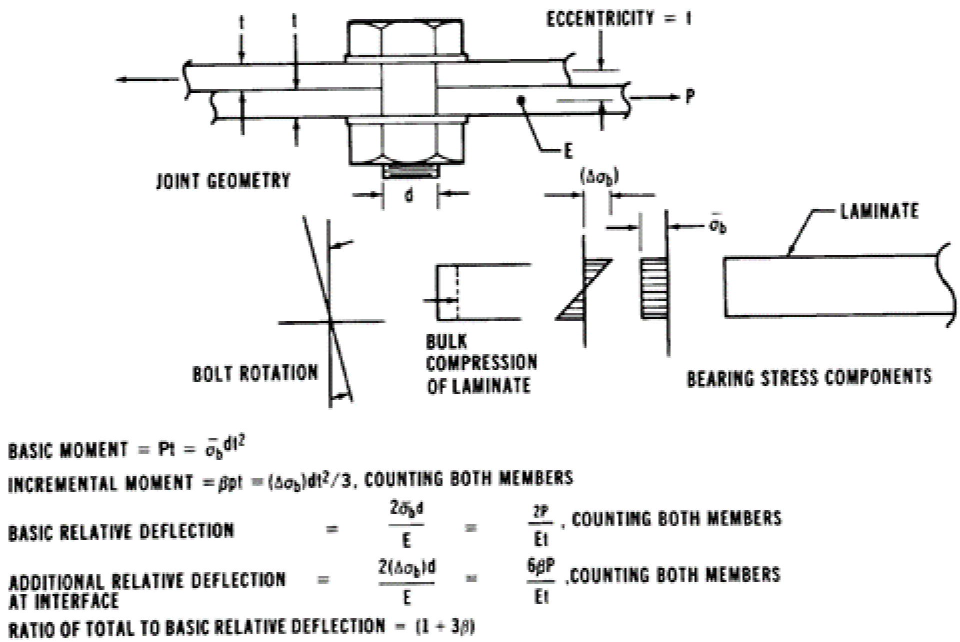

Figure 11 Additional displacements due to bolt rotation

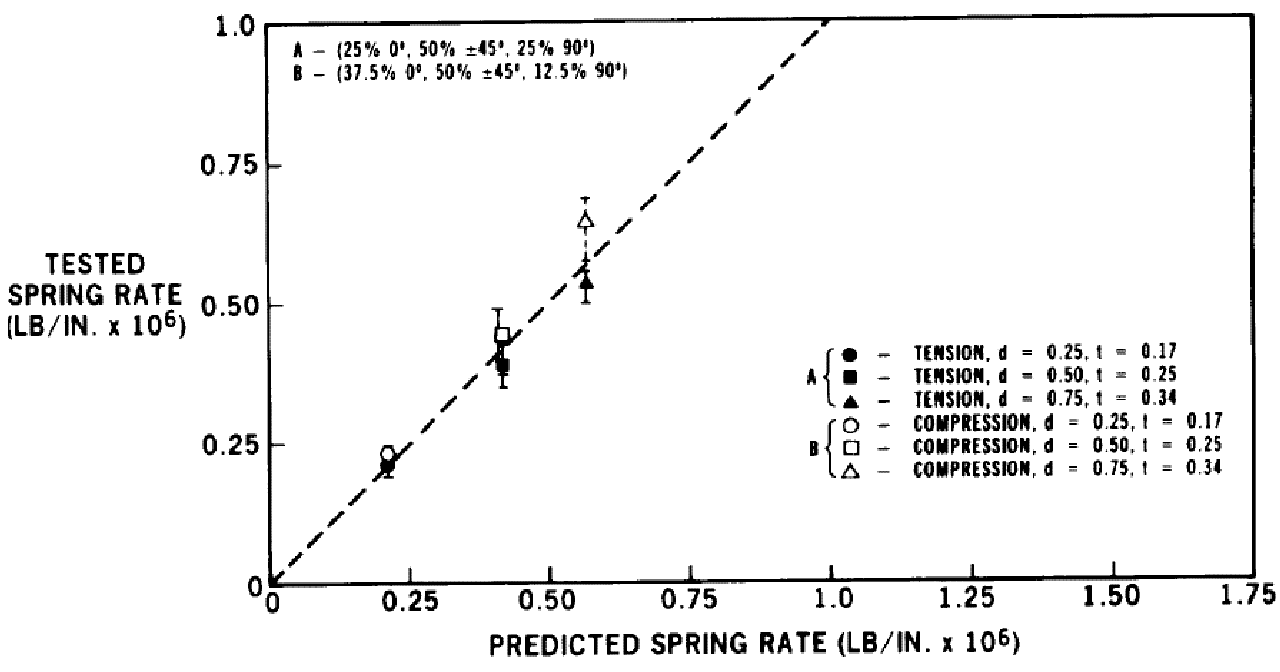

Figure 12 Single shear bolted joint elastic spring rates – test versus prediction

The actual predictions of the test results for the multirow bolted joints were based on the stiffness formulas for the elastic behavior, with the definition of the nonlinear behavior taken from the actual load deflection curves from the appropriate single-hole tests because there was often considerable deformation prior to failure.[11]

One significant finding of the single-hole tests was that, in double shear, the allowable strength of the central plate was always greater than that of the splice plates despite the matched thicknesses, presumably because of the better clamp-up. Therefore, in analyzing such joints, this extra strength should be accounted for in the input data. Such data would be necessary to truly optimize the design of such joints. The undamaged central plates should be retested with stronger splices because, in this test program, most of the failures occurred in the splice plates. This usually prevented the ultimate load capacity of the basic skins from being measured in the joint areas. The few test failures of the skins suggest that the additional bearing strength is an increment of about 20 percent. That correlates well with the measured bearing strengths in which fibrous composite skins were sandwiched between steel splice plates.[11]

1.5.7. Effect of fastener flexibility on load distribution

That fastener flexibility is a factor that affects the load distribution in a bolted joint assembly is a fact that has been known for a long time. What can be interesting to discuss however, is how much the difference in flexibility from the different calculation methods (Huth, Grumman, and Barrois) impacts the load distribution, and consequently the question arises: Is it really necessary to use several different methods for calculating the fastener flexibility?

In order to address this question, the load distribution as a function of the fastener flexibility will be calculated in a simple joint geometry. Dimensions and parameters of the joint that affect the fastener stiffness calculations will be varied. The parameters that are common for the three methods of interest are the thicknesses of the plates, diameter of the fasteners, and the Young's modulus of the plates and the fasteners. To get a reasonable comparison between the methods, the proper version of each method needs to be used depending on what assumption they have been derived from.[11]

How much do the results differ if an “incorrect" method is being used, for example if the user applies the double shear version of a method on a geometry that actually has single shear loaded fasteners.

In the discussion that follows, one plate is designated with subscript “s” (indicating “strap”) and the other plate with subscript “p”. In the compatibility/equilibrium method there is a strict definition of plate and strap, illustrated in Figure 13. The other members in a double-shear joint are represented by the strap. In a single- or double-shear hardpoint, the strap is the discontinuous hardpoint member, while the plate is the member through which the remote load enters the joint. [11]

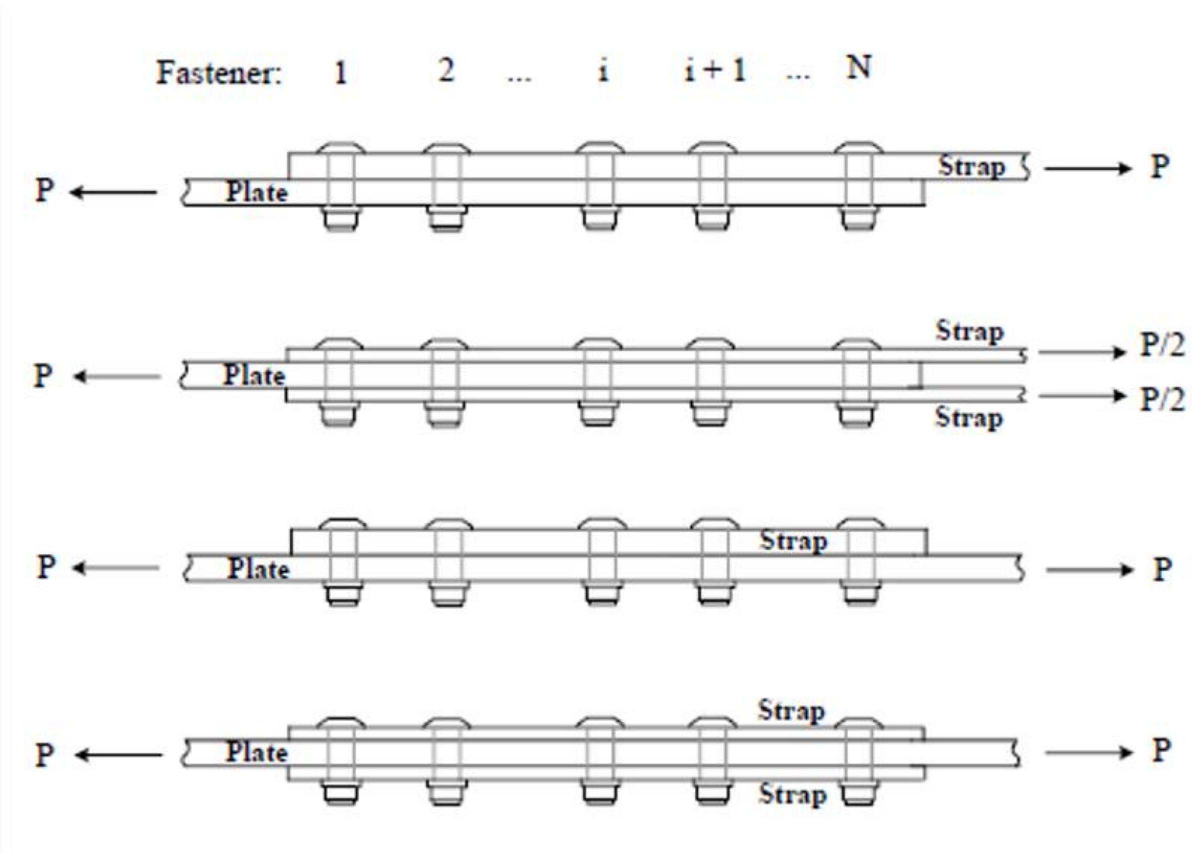

Figure 13 Terminology of plate and strap in the Compatibility/Equilibrium Method

The joint has N rows. Fasteners are numbered sequentially 1 through N. The plate load enters the joint at fastener #1, and the strap begins (has a free edge) at fastener #1.

A section of the joint, including two adjacent fasteners and the connecting plates, is isolated from the spring model, as shown in Figure 14. Deformation compatibility between points A and B states that the sum of the fastener I deformation ($\delta_{f,i}$) and strap deformation ($\delta_{s,i}$) equals the sum of the plate deformation ($\delta_{p,i}$) and the fastener i+1 deformation ($\delta_{f,(i+1)}$):

$$\delta_{f,i} + \delta_{s,i} = \delta_{p,i} + \delta_{f,(i+1)}$$

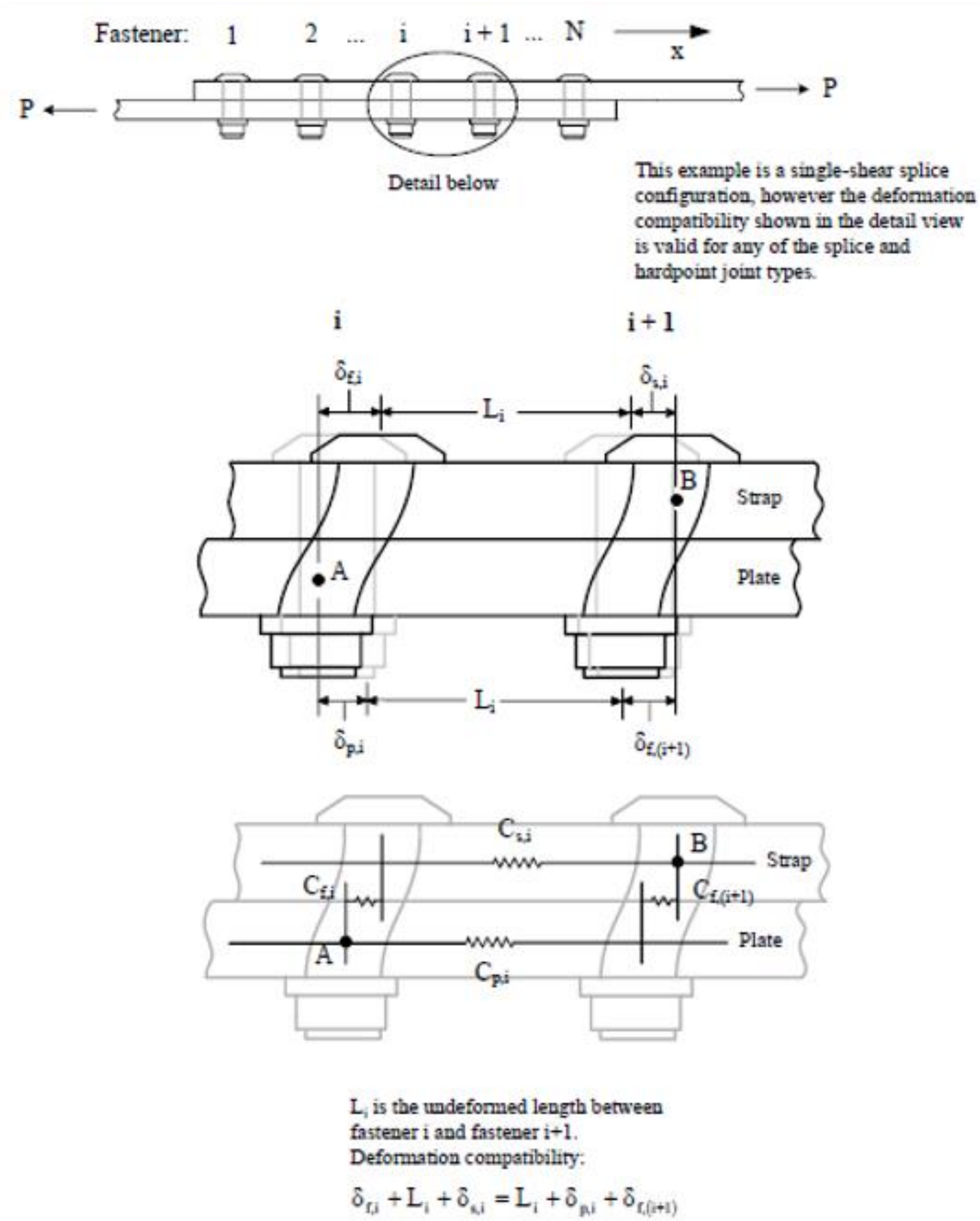

Figure 14 Deformation Compatibility between Two Adjacent Fasteners

The definition of fastener flexibility C_f is the deformation of the fastener divided by the load transferred across the fastener shear plane. Solving for deformation, for i^{th} fastener,

$$\delta_{f,i} = \left(\frac{R_i}{k}\right) C_{f,i}$$

Single shear: k=1

Symmetric double shear: k=2

Where R is the load transferred across the fastener shear plane and $C_{f,I}$ is the flexibility of the i^{th} fastener element. Note that in double-shear configurations R_i is the total load transferred through both shear planes. The definition of k (1 for single-shear, 2 for symmetric double shear) holds throughout this derivation.[11]

For the i^{th} plate element, flexibility $C_{p,I}$ is the deformation of the plate element divided by the load in the load in the plate element, therefore:

$$\delta_{p,i} = P_{p,i} C_{p,i}$$

And similarly,

$$\delta_{s,i} = P_{s,i} C_{s,i}$$

The load in the i^{th} plate element in the plate ($P_{p,i}$) and strap ($P_{s,i}$) can be determined by taking a free body of the plate and strap, cut between the i^{th} and $(i+1)^{th}$ fasteners. These free bodies are shown in Figure 15. In the strap,

$$P_{s,i} = \sum_{j=1}^{i} \left(\frac{R_j}{k}\right)$$

And in the plate,

$$P_{p,i} = P - \sum_{j=1}^{i} R_j$$

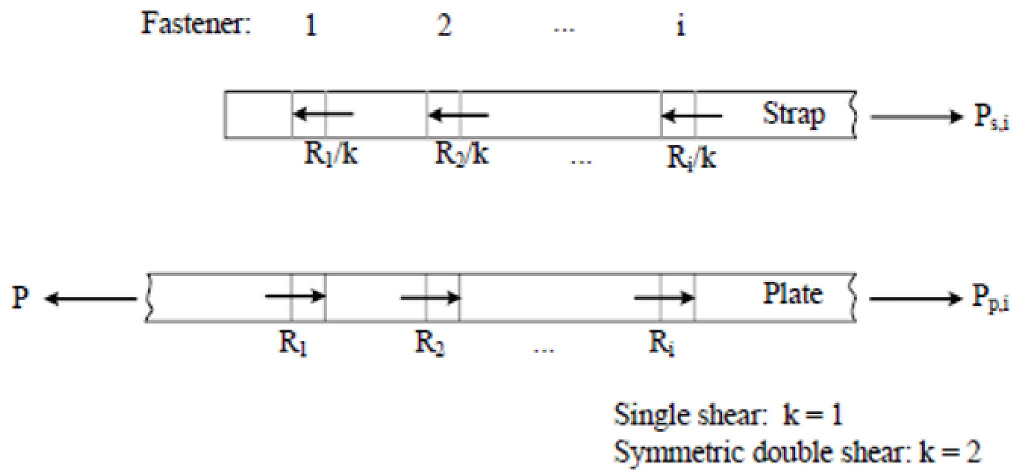

Figure 15 A free body of the plates cut past the i^th fastener

In a hardpoint, under a positive tensile load P, load transferred from the plate to strap is assigned a positive value, and load transferred from the strap to plate is assigned a negative value. A negative compressive load P reverses the sign of the R_i fastener loads. (Figure 15 shows the positive sign convention). The following equation shows the function of the unknown fastener loads (R_1 through R_i), the plate and fastener flexibility, and the applied load P:

$$\left(\frac{R_i}{k}\right) C_{f,i} + \left[\sum_{j=1}^{i} \left(\frac{R_j}{k}\right)\right] C_{s,i} = \left(P - \sum_{j=1}^{i} R_j\right) C_{p,i} + \left(\frac{R_{(i+1)}}{k}\right) C_{f,(i+1)}$$

Collecting the fastener load terms and dividing by the plate i flexibility,

$$\left(\frac{C_{f,i} + C_{s,i}}{kC_{p,i}} + 1\right) R_i + \left(\frac{C_{s,i}}{kC_{p,i}} + 1\right) \sum_{j=1}^{(i-1)} R_j - \left(\frac{C_{f,(i+1)}}{kC_{p,i}}\right) R_{(i+1)} = P$$

This equation may be written for each pair of adjacent fasteners, for a total of (N-1) equations, where N is the number of fastener rows in the single-column joint.

One additional equation can be written according to equilibrium of load in the joint, using a free body similar to Figure 15. In a lap joint, the sum of the loads across the fastener shear planes must balance the incoming load P. In a hardpoint, the incoming and outgoing loads in the strap must sum to zero.

The equations above can be assembles into a matrix that can be solved for the fastener loads R_i:

$$\begin{bmatrix} D_1 & B_1 & 0 & 0 & \cdots & 0 & 0 \\ A_2 & D_2 & B_2 & 0 & \cdots & 0 & 0 \\ A_3 & A_3 & D_3 & B_3 & \cdots & 0 & 0 \\ \vdots & \vdots & \vdots & \vdots & \cdots & \vdots & \vdots \\ A_{(N-1)} & A_{(N-1)} & A_{(N-1)} & A_{(N-1)} & \cdots & D_{(N-1)} & B_{(N-1)} \\ 1 & 1 & 1 & 1 & \cdots & 1 & 1 \end{bmatrix} \begin{bmatrix} R_1 \\ R_2 \\ R_3 \\ R_4 \\ \vdots \\ R_{(N-1)} \\ R_N \end{bmatrix} = \begin{bmatrix} P \\ P \\ P \\ \vdots \\ P \\ \langle 0 \text{ or } P \rangle \end{bmatrix}$$

(The last row of the right-hand side is 0 for a hardpoint, and P for a lap joint).

Term is the matrix are:

$$A_i = \frac{C_{s,i}}{kC_{p,i}} \qquad B_i = \frac{-C_{f,(i+1)}}{kC_{p,i}} \qquad D_i = \frac{C_{f,i}+C_{s,i}}{kC_{p,i}} + 1$$

Where k = 1 for single-shear joints, and k = 2 for symmetric double-shear joints.

2. Calculation fastener flexibility in single shear joint

2.1. Rigidity determination of composites

Each of individual layer (lamina) consists of unidirectional fibers, which determine the direction of the layer and a matrix that provides normal and transverse stiffness of the layer. This lamina is orthotropic, since it has two reciprocal axes of symmetry. The characteristic feature is that normal stresses which act along the orthotropic axes don`t cause shear deformations and tangential stresses don`t cause elongations. Hooke`s law, which describes the stress-strain relation for unidirectional lamina in a plain stress-strain state is defined as:

$$\begin{Bmatrix} \sigma_1 \\ \sigma_2 \\ \tau_{12} \end{Bmatrix} = \begin{bmatrix} C_{11}^0 & C_{12}^0 & 0 \\ C_{12}^0 & C_{22}^0 & 0 \\ 0 & 0 & C_{66}^0 \end{bmatrix} \cdot \begin{Bmatrix} \varepsilon_1 \\ \varepsilon_2 \\ \gamma_{12} \end{Bmatrix}$$

Where:

σ_1, σ_2, τ_{12} – stresses which act on lamina;

ε_1, ε_2, γ_{12} – strains of lamina;

C_{kl}^0 - lamina`s coefficients of matrix of rigidity, which define:

$$C_{11}^0 = \frac{E_1}{1-\mu_{12}\cdot\mu_{21}} \qquad C_{12}^0 = \frac{E_1\cdot\mu_{21}}{1-\mu_{12}\cdot\mu_{21}} = \frac{E_2\cdot\mu_{12}}{1-\mu_{12}\cdot\mu_{21}} \qquad C_{22}^0 = \frac{E_2}{1-\mu_{12}\cdot\mu_{21}} \qquad C_{66}^0 = G_{12}$$

Where:

E_1, E_2 – longitudinal and transverse modules of elasticity for lamina;

G_{12} – lamina shear modulus;

μ_{12} – principal Poisson`s coefficient

μ_{21} – minor Poisson`s coefficient which determined from Maxwell relation:

$$\mu_{12} \cdot E_2 = \mu_{21} \cdot E_1$$

Typical elastic characteristics of carbon and carbon fabric laminas are presented in the Table 3

Lamina	Elastic and shear modulus, psi			Poisson`s coefficients	
	E_1	E_2	G_{12}	μ_{12}	μ_{21}
Tape	2.1E7	1.2E6	8.1E5	0.36	0.021
Fiber	9.4E6	9.1E6	9.4E5	0.07	0.068

Table 3 Elastic characteristics of laminas

Tape

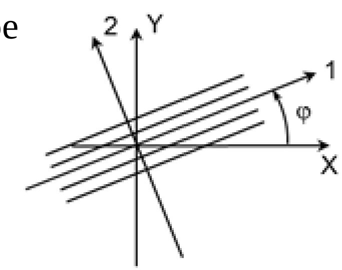

Fiber direction

Fabric

Weft direction

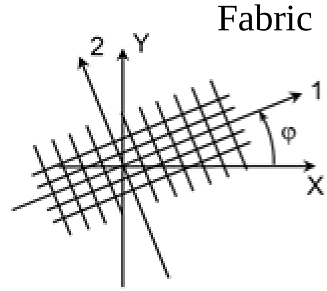

Warp direction

Figure 16 Lamina rotated by an angle φ with respect to the coordinate system of the laminate

If the loading of the lamina doesn`t occur along the orientation axis, then it is in the state of layer-by-layer loading as part of the PCM package. Then Hooke`s law takes the form:

$$\begin{Bmatrix} \sigma_x \\ \sigma_y \\ \tau_{xy} \end{Bmatrix} = \begin{bmatrix} C_{11}^{\varphi} & C_{12}^{\varphi} & C_{16}^{\varphi} \\ C_{13}^{\varphi} & C_{22}^{\varphi} & C_{26}^{\varphi} \\ C_{16}^{\varphi} & C_{26}^{\varphi} & C_{66}^{\varphi} \end{bmatrix} \cdot \begin{Bmatrix} \varepsilon_x \\ \varepsilon_y \\ \gamma_{xy} \end{Bmatrix}$$

Where lamina`s coefficients of matrix of rigidity rotated by an angle φ (see Figure 16)

$$C_{11}^{\varphi} = V_1 + V_2 \cdot \cos 2\varphi + V_3 \cdot \cos 4\varphi;$$

$$C_{12}^{\varphi} = V_1 - 2 \cdot V_4 - V_3 \cdot \cos 4\varphi;$$

$$C_{16}^{\varphi} = 0.5 \cdot V_2 \cdot \sin 2\varphi + V_3 \cdot \sin 4\varphi;$$

$$C_{22}^{\varphi} = V_1 - V_2 \cdot \cos 2\varphi + V_3 \cdot \cos 4\varphi;$$

$$C_{26}^{\varphi} = 0.5 \cdot V_2 \cdot \sin 2\varphi - V_3 \cdot \sin 4\varphi;$$

$$C_{66}^{\varphi} = V_4 - V_3 \cdot \cos 4\varphi.$$

$i(\phi)$	C_{11}^{i}	C_{12}^{i}	C_{16}^{i}	C_{22}^{i}	C_{26}^{i}	C_{66}^{i}
0	20899502	441959	0	1227663	0	812211
15	18457088	1566609	4406931	1420776	511029	1936861
30	12607592	3815909	6207029	2771672	2311127	4186162
45	6564982	4940559	4917960	6564982	4917960	5310812
60	2771672	3815909	2311127	12607592	6207029	4186162
75	1420776	1566609	511029	18457088	4406931	1936861
90	1227663	441959	0	20899502	0	812211
-15	18457088	1566609	-4406931	1420776	-511029	1936861
-30	12607592	3815909	-6207029	2771672	-2311127	4186162
-45	6564982	4940559	-4917960	6564982	-4917960	5310812
-60	2771672	3815909	-2311127	12607592	-6207029	4186162
-75	1420776	1566609	-511029	18457088	-4406931	1936861

Table 4 Lamina`s coefficients of matrix of rigidity for tape rotated by an angle φ

$i(\phi)$	C_{11}^{i}	C_{12}^{i}	C_{16}^{i}	C_{22}^{i}	C_{26}^{i}	C_{66}^{i}
0	9472440	642669	0	9180980	0	942745
15	8603097	1492487	1508362	8350685	-1435497	1792564
30	6850118	3192125	1535032	6704388	-1408827	3492202
45	5927435	4041944	72865	5927435	72865	4342021
60	6704388	3192125	-1408827	6850118	1535032	3492202
75	8350685	1492487	-1435497	8603097	1508362	1792564
90	9180980	642669	0	9472440	0	942745
-15	8603097	1492487	-1508362	8350685	1435497	1792564
-30	6850118	3192125	-1535032	6704388	1408827	3492202
-45	5927435	4041944	-72865	5927435	-72865	4342021
-60	6704388	3192125	1408827	6850118	-1535032	3492202
-75	8350685	1492487	1435497	8603097	-1508362	1792564

Table 5 Lamina`s coefficients of matrix of rigidity for fiber rotated by an angle φ

Here the independent coefficients V_1, V_2, V_3 and V_4 are determined:

$$V_1 = \left(3 \cdot C_{11}^0 + 2 \cdot C_{12}^0 + 3 \cdot C_{22}^0 + 4 \cdot C_{66}^0\right)/8;$$
$$V_2 = \left(C_{11}^0 - C_{22}^0\right)/2;$$
$$V_3 = \left(C_{11}^0 - 2 \cdot C_{12}^0 + C_{22}^0 - 4 \cdot C_{66}^0\right)/8;$$
$$V_4 = \left(C_{11}^0 - 2 \cdot C_{12}^0 + C_{22}^0 + 4 \cdot C_{66}^0\right)/8.$$

Lamina	V1	V2	V3	V4
Tape	7627072	145730	1699638	3E+06
Fiber	8814282	9835919	2249300	3E+06

Table 6 Independent coefficients for tape and fiber

Coefficients V_1 and V_4 characterize the average stiffness of the lamina under tension and shear and coefficients V_2 and V_3 characterize the degree of anisotropy of the material.

Thus, the behavior of a lamina in a plain stress-strain state is characterized by four independent elastic constants:

E_1, E_2, G_{12}, μ_{12} – for angles of reinforcing 0° and 90°;

V_1, V_2, V_3, V_4 – for angles of reinforcing φ°.

Elastic characteristics of a lamina rotated by an angle φ

$$E_x = \frac{\Delta C}{C_{22}^{\varphi} \cdot C_{66}^{\varphi} - (C_{26}^{\varphi})^2}; \qquad G_{xy} = \frac{\Delta C}{C_{11}^{\varphi} \cdot C_{22}^{\varphi} - (C_{12}^{\varphi})^2};$$

$$E_y = \frac{\Delta C}{C_{11}^{\varphi} \cdot C_{66}^{\varphi} - \left(C_{16}^{\varphi}\right)^2}; \qquad \mu_{xy} = \frac{C_{12}^{\varphi} \cdot C_{66}^{\varphi} - C_{16}^{\varphi} \cdot C_{26}^{\varphi}}{C_{22}^{\varphi} \cdot C_{66}^{\varphi} - (C_{26}^{\varphi})^2},$$

Where ΔC – is a determinant of matrix of rigidity

$$\Delta C = \det \begin{bmatrix} C_{11}^{\varphi} & C_{12}^{\varphi} & C_{16}^{\varphi} \\ C_{12}^{\varphi} & C_{22}^{\varphi} & C_{26}^{\varphi} \\ C_{16}^{\varphi} & C_{26}^{\varphi} & C_{66}^{\varphi} \end{bmatrix}$$

For layup ±φ elastic characteristics for layup ±φ are equel:

	#	$\phi(^o)$	E_x (psi)	E_y (psi)	G_{xy} (psi)	μ_{xy}
Fiber	1	0	9427453	9137378	942745	0.07
	2	±15	8336350	8091765	1792564	0.18
	3	±30	5330269	5216872	3492202	0.48
	4	±45	3171215	3171215	4342021	0.68
	5	±60	5216872	5330269	3492202	0.47
	6	±75	8091765	8336350	1792564	0.17
	7	90	9137378	9427453	942745	0.07
Tape	1	0	20740397	1218317	812211	0.36
	2	±15	16729678	1287805	1936861	1.10
	3	±30	7354026	1616720	4186162	1.38
	4	±45	2846902	2846902	5310812	0.75
	5	±60	1616720	7354026	4186162	0.30
	6	±75	1287805	16729678	1936861	0.08
	7	90	1218317	20740397	812211	0.02

Table 7 Elastic properties for lamina rotated by an angle ϕ

Changes in the elastic and shear modulus of the fiber Figure 17 and tape Figure 18 depending on the angle φ

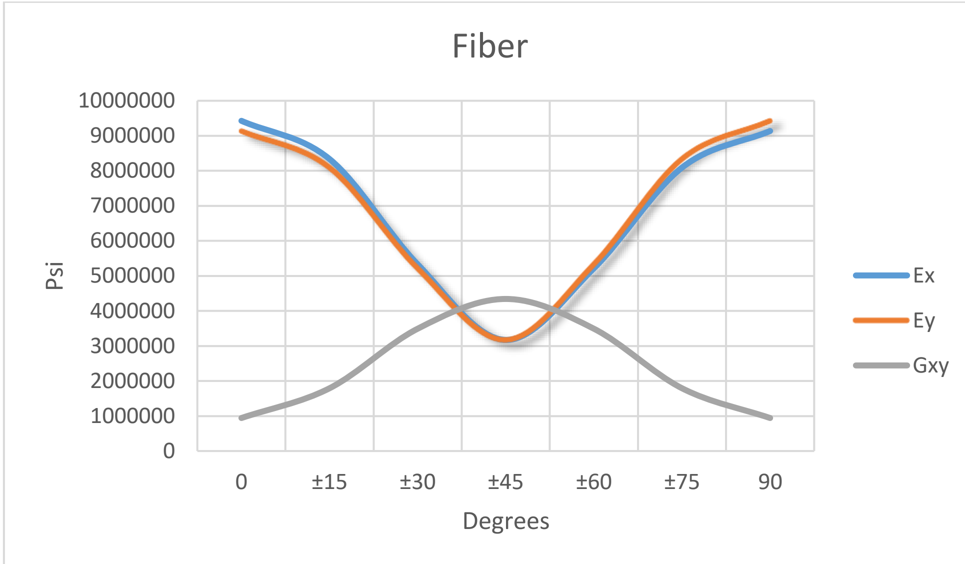

Figure 17 Elastic and shear modulus for the fiber depending on the angle φ

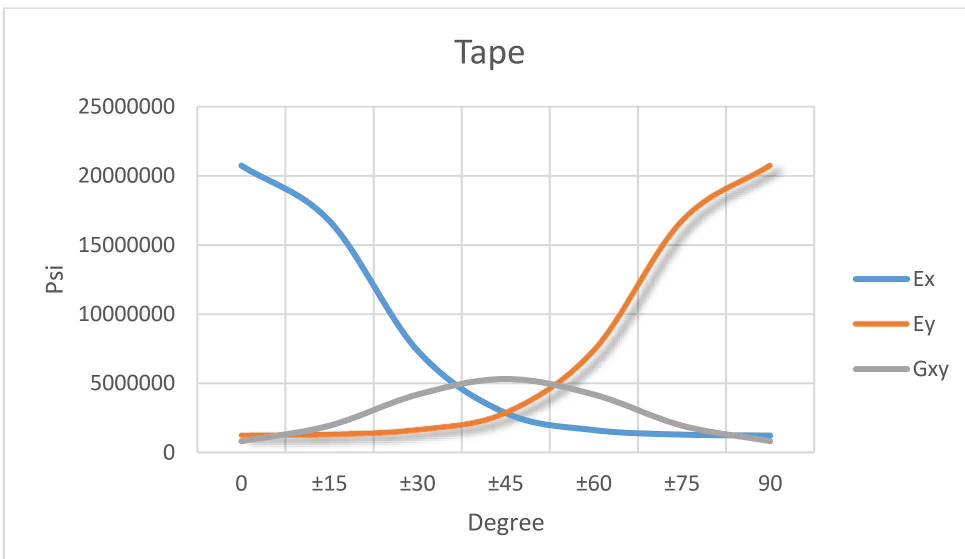

Figure 18 Elastic and shear modulus for the tape depending on the angle φ

Changes in the elastic and shear modulus of the carbon fabric and tape depending on the angle φ which presented in Figure 17 Figure 18

2.2. Method Tate

To calculate fastener flexibility the following formula was used. It takes account effect of shear, bending and bearing of bolt.

$$C_i = C_{bs} + C_{bb} + C_{br} + C_{pbr}$$

Where bolt shear effect is:

$$C_{bs} = \frac{2t_s + t_p}{3G_b A_b}$$

Bolt bending effect is:

$$C_{bb} = \frac{8t_s^3 + 16t_s^2 t_p + 8t_s t_p^2 + t_p^3}{192E_{bb} I_b}$$

Bolt bearing effect is:

$$C_{bbr} = \frac{2t_s + t_p}{t_s t_p E_{bbr}}$$

Plate bearing effect is:

$$C_{pbr} = \frac{1}{t_s E_{sbr}} + \frac{2}{t_p E_{pbr}}$$

Input data:

Fastener material – Ti-6Al-4V

E_f = 1.6E7 psi – elastic modulus for fastener

G_f = 6.2E6 psi – shear modulus for fastener

Strap material – Aluminum

E_s = 1.0E7 psi – elastic modulus for strap

Plate material CFRP

E_p = 8.6E6 psi – modulus of elasticity for composite material

Geometrical parameters:

d = 0.25 in – diameter of bolts

t_s = 0.148 in – thickness of the aluminum strap

t_p = 0.148 in – thickness of the composite plate

$$I_b = \frac{\pi \cdot d^4}{64} = \frac{3{,}14 \cdot 0{,}25^4}{64} = 0{,}00019\ in^4 - \text{moment of inertia of fastener}$$

$$A_b = \frac{\pi \cdot d^2}{4} = \frac{3{,}14 \cdot 0{,}25^2}{4} = 0.05\ in^2 - \text{area of fastener}$$

p = 1.25 in – distance between fasteners in longitudinal direction

w = 1.25 in – distance between fasteners in transverse direction

Calculation of fastener flexibility, see table

Ci	4.18456E-06
Cbs	4.86295E-07
Cbb	1.81613E-07
Cbbr	1.26689E-06
Cpbr	2.24976E-06

Table 8 Calculation of i^{th} fastener flexibility

2.3. Method Huth

Based on extensive testing on different types of joints and materials, a formula for fastener flexibility was fitted to load-displacement curves as

$$f = \left(\frac{t_1 + t_2}{2d}\right)^a \frac{b}{n}\left(\frac{1}{E_1 t_1} + \frac{1}{nE_2 t_2} + \frac{1}{2E_f t_1} + \frac{1}{2nE_f t_2}\right)$$

Input data:

For material and geometric parameters see part “Rigidity determination of composites” n = 1 – coefficient for single shear

a = 0.67 – the impiric values which is taken from the figure below

b = 4.2 – the impiric values which is taken from the figure below

Single shear	$n = 1$
Double shear	$n = 2$
Bolted metallic joints	$a = 2/3,\ b = 3.0$
Riveted metallic joints	$a = 2/5,\ b = 2.2$
Bolted graphite/epoxy joints	$a = 2/3,\ b = 4.2$

Figure 19 Huth parameters

f = 5.58E-6 1/in psi – fastener flexibility using method Huth.

2.4.Fastener modeling for MSC. Nastran finite element analysis

2.4.1. Stiffness of fastener joint

In a fastener joint Figure 20 the following stiffness components are considered:

- translational plate bearing stiffness;
- translational fastener bearing stiffness;
- rotational plate bearing stiffness;
- rotational fastener bearing stiffness;
- fastener shear stiffness;
- fastener bending stiffness.

Under load, the plates slide relative to each other. This causes the translational bearing deformations of joined plates and a fastener. The translational bearing flexibility of plate *i* is:

$$C_{btp_i} = \frac{1}{E_{cp_i} t_{p_i}}$$

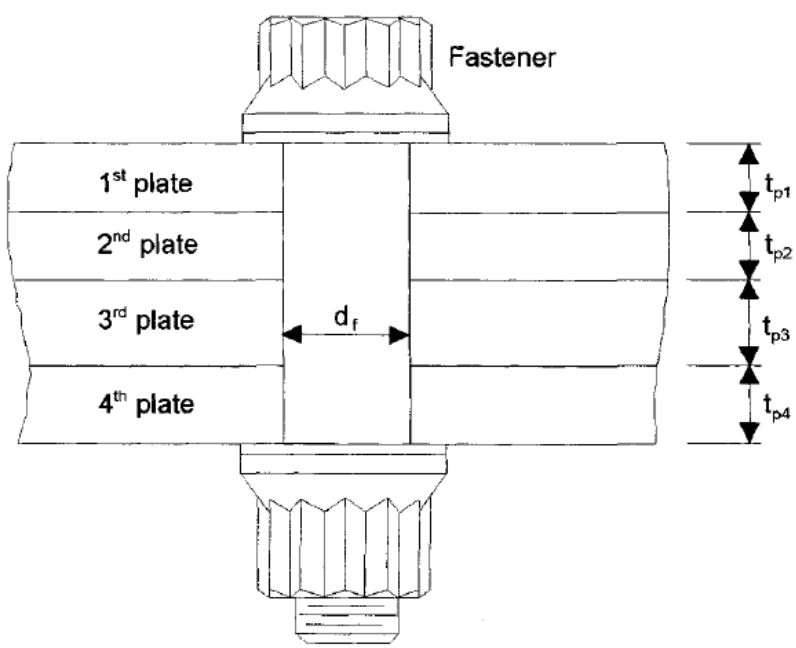

Figure 20 Fastener joint

Where:

E_{cpi} – compression modulus of plate *I* material;

t_{pi} – thickness of plate *i*.

The fastener translational bearing flexibility at plate *i:*

$$C_{btf_i} = \frac{1}{E_{cf} t_{p_i}}$$

Where :

E_{cf} – compression modulus of fastener material

Combined fastener and plate translational bearing flexibility at plate i

$$C_{bt_i} = C_{btp_i} + C_{btf_i}$$

Combined translational bearing stiffness at plate *i*

$$S_{bt_i} = \frac{1}{C_{bt_i}}$$

The relative rotation of the plate and fastener creates a moment in the plate-fastener interaction (Figure 21). The bearing deformations caused by this relative rotation are assumed distributed linearly along the plate thickness

$$\delta = x\varphi$$

Where

x – coordinate along the plate thickness;

ϕ – angle of relative rotation of the plate and fastener

Stiffness of a dx thick slice of plate *i* is:

$$dS_{btp_i} = E_{cp_i} dx$$

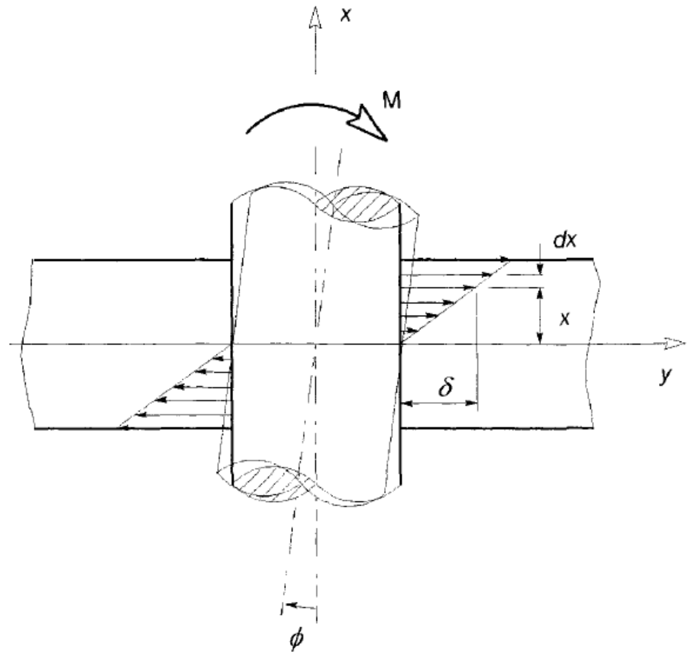

Figure 21 Rotation bearing stiffness definition

Load on dx thick slice of plate / caused by the plate bearing deformation

$$dF = \delta dS_{btp_i} = x\varphi E_{cp_i} dx$$

Moment of dF force about the plate *i* center line

$$dM = xdF = \varphi E_{cp_i} x^2 dx$$

Moment in the plate fastener contact caused by the plate deformation

$$M = E_{cp_i}\varphi \int_{-\frac{t_{p_i}}{2}}^{\frac{t_{p_i}}{2}} x^2 dx = E_{cp_i}\varphi \frac{t_{p_i}^3}{12}$$

The rotation bearing flexibility of a plate *i*

$$C_{brf_i} = \frac{\varphi}{M} = \frac{12}{E_{cp_i} t_{p_i}^3}$$

The fastener rotation bearing flexibility at plate *i*

$$C_{brp_i} = \frac{12}{E_{cf_i} t_{p_i}^3}$$

Combined fastener and plate rotation bearing flexibility at plate *i*

$$C_{br_i} = C_{brp_i} + C_{brf_i}$$

Combined rotational bearing stiffness at plate *i*

$$S_{br_i} = \frac{1}{C_{br_i}}$$

The bearing stiffness is modeled by elastic elements. The shear and bending stiffness of a fastener are represented by a beam element.

2.4.2. Modeling of a fastener joint

Modeling of a fastener joint is illustrated here using MSC. Nastran.

Idealization of a plate-fastener system includes the following:

- Elastic bearing stiffness of a plate and fastener at contact surface;
- Bending and shear stiffness of a fastener shank;
- Compatibility of displacements of a fastener and connected plates at the joint.

The presented method creates the plate-fastener system illustrated in Figure 22

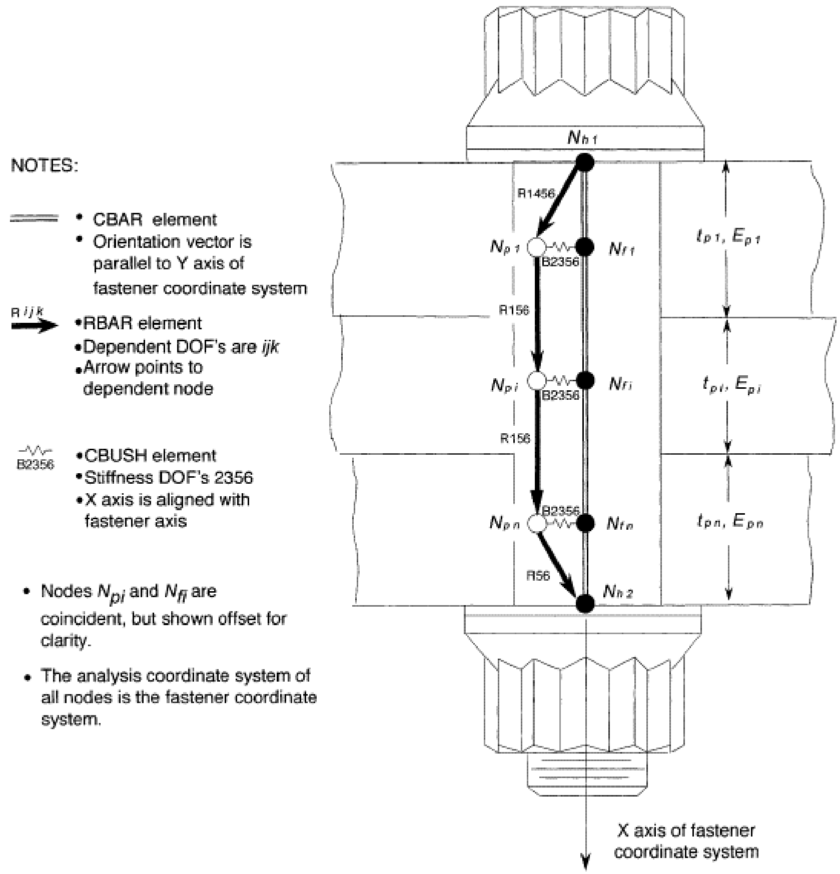

Figure 22 Fastener joint modeling

A fastener is modeled by CBAR or CBEAM elements with corresponding PBAR or PBEAM cards for properties definition. For the CBAR or CBEAM elements connectivity, a separate set of grid points coincidental with corresponding plate grid points (Figure 3) is created. This set also includes grid points located on intersection of the fastener axis and outer surfaces of the first and last connected plates.

All CBAR or CBEAM elements representing the same fastener reference the same PBAR or PBEAM card with following properties:

- MID to reference the fastener material properties;
- Fastener cross section area

$$A = \frac{\pi d_f^2}{4}$$

Where

d_f – fastener diameter

- Moment of inertia of the fastener cross section

$$I_1 = I_2 = \frac{\pi d_f^4}{64}$$

- Torsion constant

$$J = \frac{\pi d_f^4}{32}$$

- Area factor for shear of circular section

K_1=K_2=0.9

The interaction between a fastener and plate results in bearing deformation of all parts of the joint on their surfaces of contact. The bearing stiffness of a fastener and connected plates is defined in Section "Stiffness of fastener joint". The bearing stiffness is presented as translational stiffness in direction of axes normal to the fastener axis and defining the fastener shear plane and rotational stiffness about the same axes.

For the modeling of the bearing stiffness, two sets of coincident grid points mentioned above are used. Each pair of coincident grid points, i.e. the plate node and corresponding fastener node, is connected by CBUSH element [2] or combination of CELAS2 elements with equal translational stiffness along the axes normal to the fastener axis and equal rotational stiffness about the same axes. The connectivity card CBUSH must be accompanied by PBUSH card defining the stiffness. The CELAS2 card accomplishes both functions, but 4 CELAS2 elements are required to replace one CBUSH element. However it is difficult to interpret CELAS2 element forces.

For correct definition of a fastener shear plane and its axial direction, a coordinate system with one of its axis parallel to the fastener axis must be defined in the bulk data. This coordinate system must be used as analysis coordinate system for both sets of grid points.

2.4.3. Compatibility of displacements in the joint

The fastener joint model was designed under the following assumptions:

- The plates are incompressible in transverse direction;
- The plates mid planes stay parallel to each other under the load;
- Planes under the fastener heads stay parallel to the plate mid planes under the load.

These goals are reached by using REAR elements. The first RBAR card forces the plane under the fastener head to stay parallel to the first plate mid plane under the load. It also prevents the fastener movement as a rigid body. The middle RBAR cards support the first two assumptions. They keep the constant distance between the plate mid planes, i.e. assume that plates are incompressible. They also guarantee zero relative rotation of plates keeping them parallel to each other. The last card forces the plane under the other head of the fastener to stay parallel to the last plate mid plane.

2.4.4. Modeling

A single shear joint was modelled as an experiment to compare results of diploma with FEA analysis. The modeled structure consists of composite plate, aluminum strap and three fasteners (see Figure 23). The thickness is 0.148 for plate and for strap (see Figure 24). The aluminum strap is loaded by a distributed load of 800 lb/in (total load = w*q = 1.25*800 = 1000 lb, where w – width of strap), see Figure 25. The model is constrained at edge as fixed. To model fastener the fastener builder utility was used. The starting ID of the new nodes and elements can be selected, as it is usually done in majority of input forms. On the symmetry coefficient panel the user has three choice:

- 1.0 – for fasteners not located on symmetry planes;
- 0.5 – for fasteners belonging to one plane of symmetry
- 0.25 – for fasteners located on the intersection of symmetry planes.

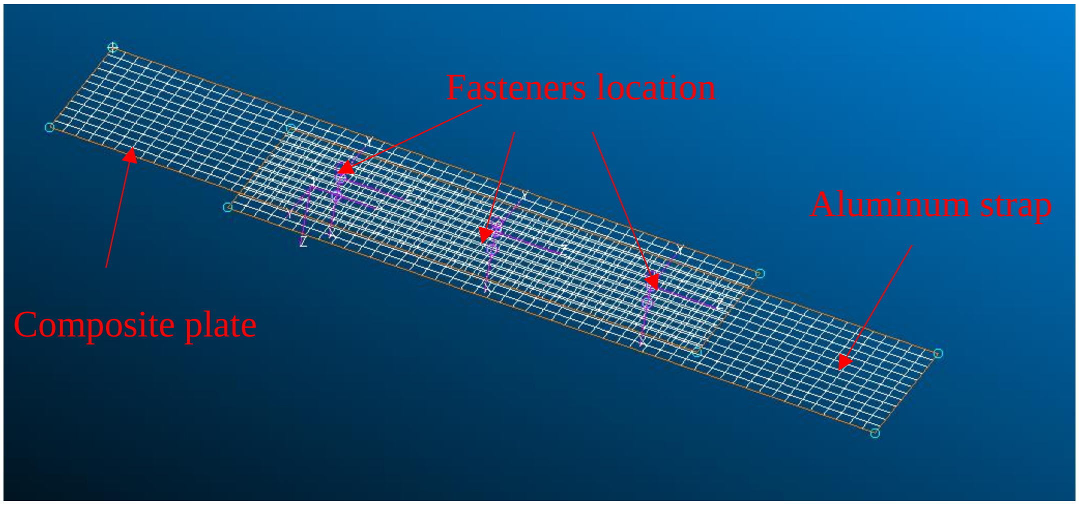

Figure 23 Single shear joint in Patran

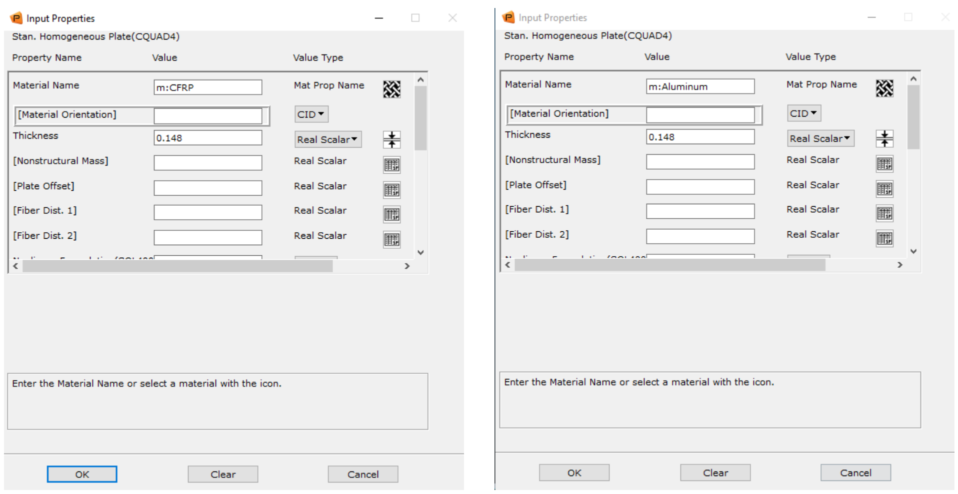

Figure 24 Thickness of the plate and strap

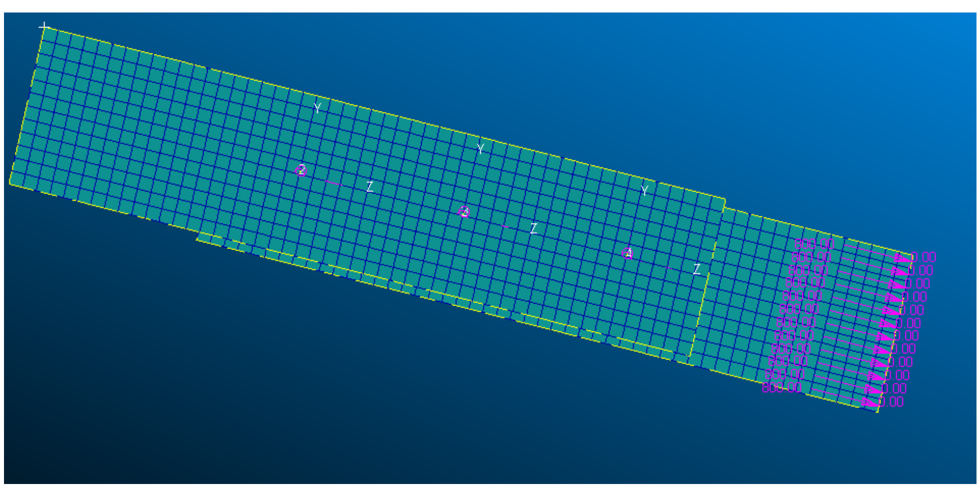

Figure 25 Distributed load

In our case the fasteners are on a symmetry plane, the coordination system has to be identified. Analysis was calculated by Nastran, and result is shown in the Figure 26.

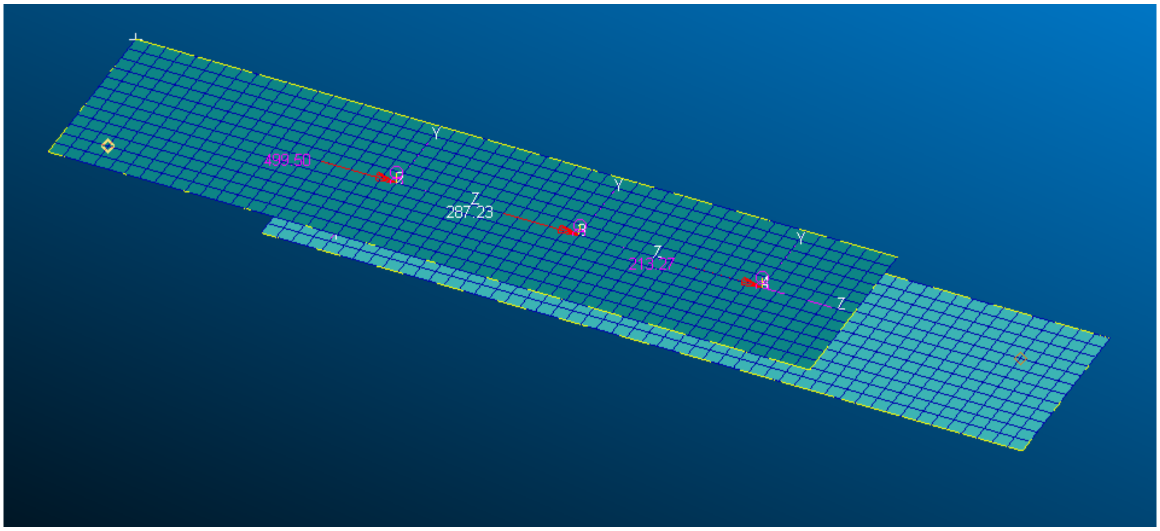

Figure 26 Result of load distribution

2.5.Load distribution between fasteners

It`s already known the fastener flexibility so let`s determine the load distribution between fasteners. For example, let`s check the several variants: load distribution between 2,3,4,5,6 fasteners in a row.

For theory see part “Effect of fastener flexibility on load distribution”.

Step 1. Calculation matrix coefficients A, B, D.

$$A_i = \frac{C_{s,i}}{kC_{pi}} + 1$$

$$B_i = \frac{-C_{f,(i+1)}}{kC_{pi}}$$

$$D_i = \frac{C_{f,i} + C_{s,i}}{kC_{pi}} + 1$$

Where:

$$C_{si} = \frac{p}{E_s t_s w}$$

$$C_{pi} = \frac{p}{E_p t_p w}$$

$C_{fi} = C_i -$ fastener flexibility determinated by different methods

	Csi	Cpi	Cfi	k	A	B	D
1	6.8E-07	7.87E-07	4.2E-06	1	1.86	-5.32	7.18
2	6.8E-07	7.87E-07	4.2E-06	1	1.86	-5.32	7.18
3	6.8E-07	7.87E-07	4.2E-06	1	1.86	-5.32	7.18
4	6.8E-07	7.87E-07	4.2E-06	1	1.86	-5.32	7.18
5	6.8E-07	7.87E-07	4.2E-06	1	1.86	-5.32	7.18
6	6.8E-07	7.87E-07	4.2E-06	1	1.86	0	7.18

Table 9 Matrix component and coefficient (Tate)

Step 2 Create a matrix taking account information above

7.6	-5.6	0	0	0	0
1.9	7.6	-5.6	0	0	0
1.9	1.9	7.6	-5.6	0	0
1.9	1.9	1.9	7.6	-5.6	0
1.9	1.9	1.9	1.9	7.6	-5.6
1.0	1.0	1.0	1.0	1.0	1.0

Table 10 Matrix of rigidity for 6 fasteners

Step 3: Determine the inverse matrix because of dividing matrix

0.10	0.06	0.03	0.02	0.01	0.04
-0.04	0.07	0.04	0.02	0.01	0.05
-0.02	-0.06	0.07	0.03	0.01	0.08
-0.01	-0.03	-0.07	0.06	0.02	0.14
-0.01	-0.02	-0.04	-0.07	0.04	0.25
-0.01	-0.02	-0.03	-0.06	-0.10	0.44

Table 11 Inverse matrix

Step 4: Multiply inverse matrix of rigidity by matrix P and gets the matrix which components are our reactions

R1 = 245.2 lb

R2 = 152.4 lb

R3 = 112.1 lb

R4 = 110.4 lb

R5 = 146.6 lb

R6 = 233.4 lb

Repeat all 4 steps for each load case (2,3,4,5,6 fasteners) and get the result table for load distribution Tate`s method.

#\Reaction	R1(lb)	R2(lb)	R3(lb)	R4(lb)	R5(lb)	R6(lb)
2	502.2	497.8				
3	354.3	300	346.7			
4	291.6	214.7	211.8	281.9		
5	261.1	173.7	146.2	169	250	
6	245.2	152.4	112.1	110.4	146.6	233.3

Table 12 Load distribution Tate`s method for all cases

To determine load distribution by Huth method, just execute all steps above and change fastener flexibility which was calculated by Tate method into Huth flexibility.

So here we have matrix coefficients and distribution of load between 2,3,4,5,6 fasteners as well.

	Csi	Cpi	Cfi	k	A	B	D
1	6.8E-07	7.2E-07	5.4E-06	1	1.9	-7.5	9.4
2	6.8E-07	7.2E-07	5.4E-06	1	1.9	-7.5	9.4
3	6.8E-07	7.2E-07	5.4E-06	1	1.9	-7.5	9.4
4	6.8E-07	7.2E-07	5.4E-06	1	1.9	-7.5	9.4
5	6.8E-07	7.2E-07	5.4E-06	1	1.9	-7.5	9.4
6	6.8E-07	7.2E-07	5.4E-06	1	1.9	0	9.4

Table 13 Matrix component and coefficient (Huth)

#\Reaction	R1(lb)	R2(lb)	R3(lb)	R4(lb)	R5(lb)	R6(lb)
2	502	498				
3	350	307	344			
4	283	223	220	275		
5	249	180	157	175	239	
6	230	156	123	121	151	220

Table 14 Load distribution Huth`s method for all cases

The next milestone of this research is to compare results from our template (Huth and Tate methods) with existing program complexes which is used at my work. Comparing will be made for all cases. Composite material was fiber because of symmetrical distribution of fastener load see Figure 27. Program complexes which I used, are programmed by Huth method, so the result have to be the same or with minimum error.

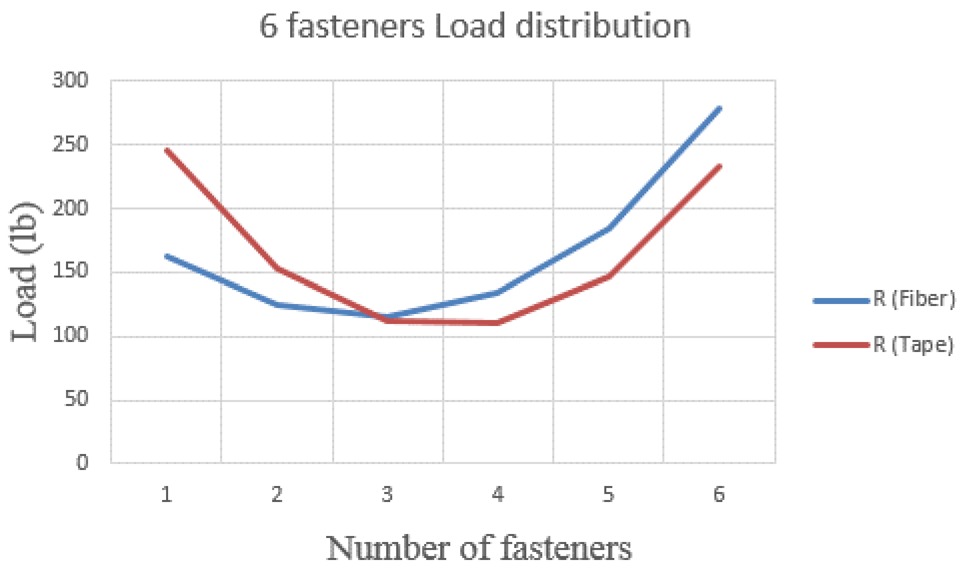

M

Figure 27 Comparing of distribution load between fiber and tape

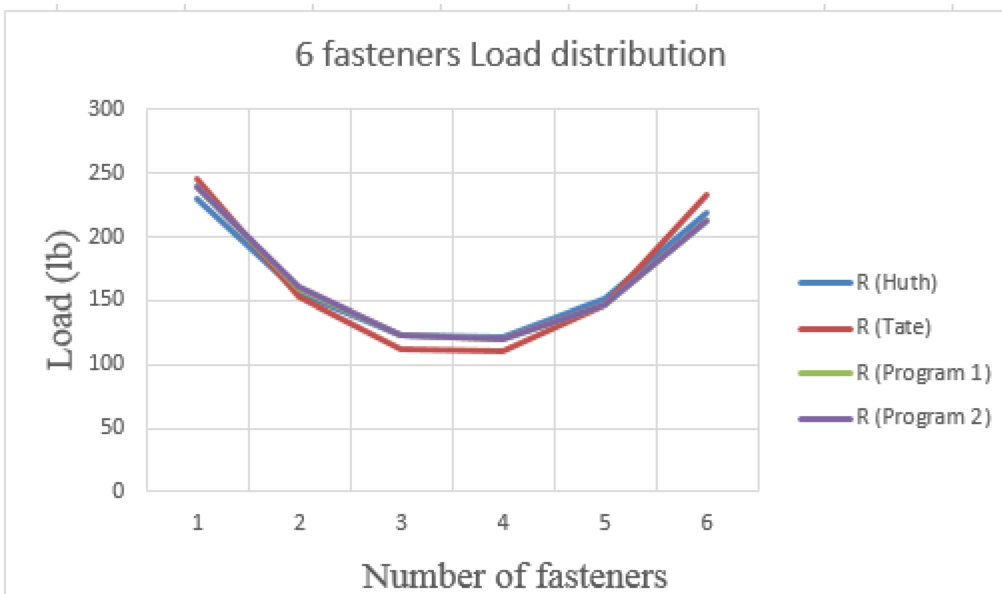

	Results using program						P (sum)
Program 1	238,6	160,0	123,5	119,4	146,5	212,0	1000,0
	23,9%	16,0%	12,4%	11,9%	14,7%	21,2%	
Program 2	238,6	160,1	123,5	119,4	146,4	212,0	1000,0
	23,9%	16,0%	12,4%	11,9%	14,6%	21,2%	
	Result using tamplate						
Tate	245,2	152,4	112,1	110,3	146,6	233,3	1000,0
	24,5%	15,2%	11,2%	11,0%	14,7%	23,3%	
Huth	229,9	156,0	122,6	121,0	150,8	219,6	1000,0
	23,0%	15,6%	12,3%	12,1%	15,1%	22,0%	

Figure 28 Comparing results for 6 fasteners

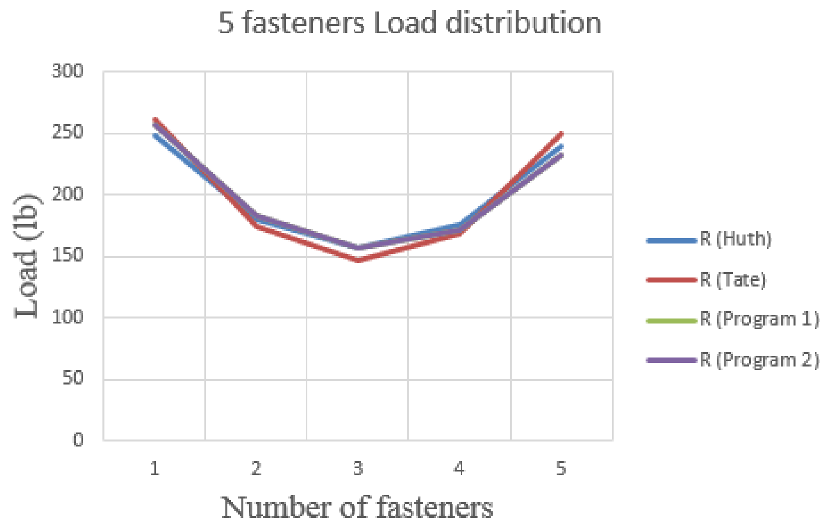

	Results using program					sum
Program 1	256,5	182,7	156,8	171,9	232,1	1000,0
	26%	18%	16%	17%	23%	
Program 2	256,5	182,7	156,8	171,9	232,1	1000,0
	26%	18%	16%	17%	23%	
	Result using tamplate					
Tate	261,1	173,7	146,2	169,0	250,0	1000,0
	26%	17%	15%	17%	25%	
Huth	248,6	179,6	157,2	175,5	239,2	1000,0
	25%	18%	16%	18%	24%	

Figure 29 Comparing results for 5 fasteners

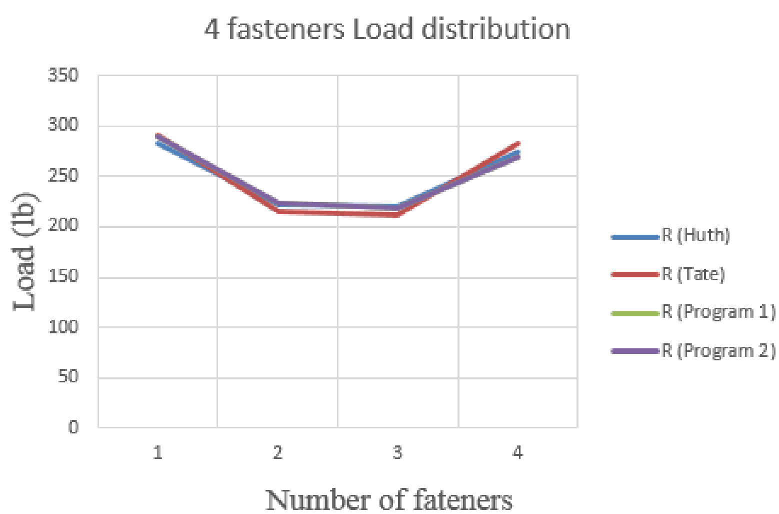

	Results using program				
Program 1	289,4	224,3	217,8	268,5	1000,0
	29%	22%	22%	27%	
Program 2	289,4	224,3	217,8	268,5	1000,0
	29%	22%	22%	27%	
	Result using tamplate				
Tate	291,6	214,7	211,8	281,9	1000,0
	29%	21%	21%	28%	
Huth	282,7	222,6	220,1	274,7	1000,0
	28%	22%	22%	27%	

Figure 30 Comparing results for 4 fasteners

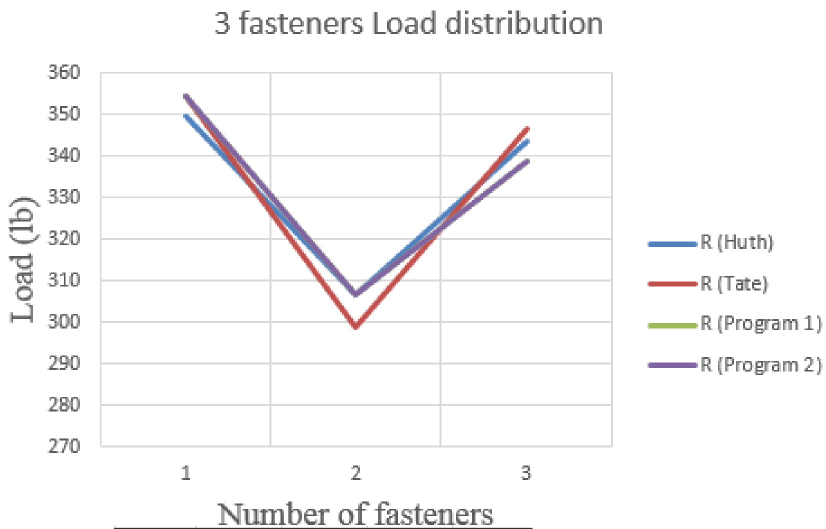

Results using program				
Program 1	354,6	306,6	338,8	1000,0
	35%	31%	34%	
Program 2	354,6	306,6	338,8	1000,0
	35%	31%	34%	
Result using tamplate				
Tate	354,3	299,0	346,7	1000,0
	35%	30%	35%	
Huth	349,6	306,8	343,6	1000,0
	35%	31%	34%	

Figure 31 Comparing results for 3 fasteners

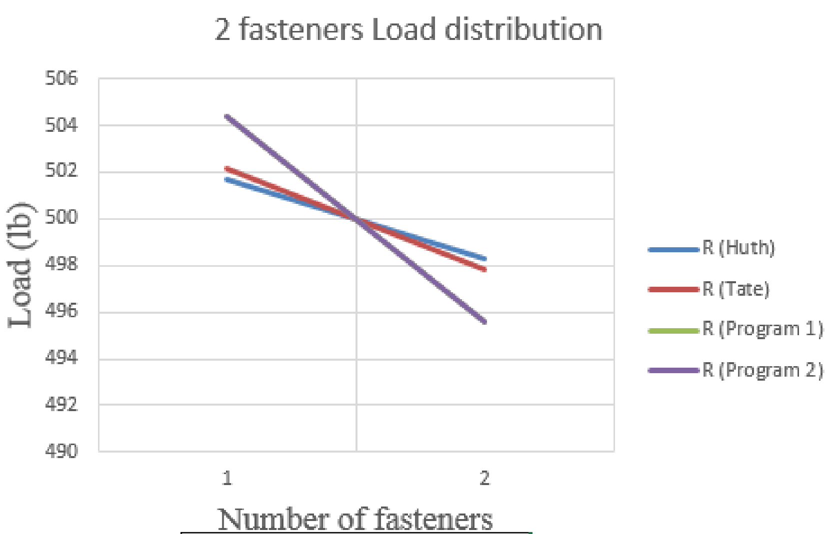

Results using program			
Program 1	504,4	495,6	1000,0
	50%	50%	
Program 2	504,4	495,6	1000,0
	50%	50%	
Result using tamplate			
Tate	502,2	497,8	1000,0
	50%	50%	
Huth	501,7	498,3	1000,0
	50%	50%	

Figure 32 Comparing results for 2 fasteners

As you can see from figures above, the error between excel template and program complexes is negligible, so template worked correctly.

3. Optimization single shear joint

This part describes optimization which means “to align” the load distribution in single shear lap joint. As we can see from previous part the load is unstable it has an extreme at first and last fasteners and very low loaded middle fasteners. Tate`s and Huth`s methods are within the margin of error, so using them in our following research and optimization are acceptable. The reason for this are additional moment from eccentricity between two plates and different elastic characteristics because of aluminum strap and composite plate. So our task is to distribute load evenly (divide into same parts).

In our optimization we will change thickness of the aluminum strap, because it`s difficult to make CFRP with tapered thickness, the reason for this is unusual construction of composite. Also we also can change the bolt diameter.

Note: In this optimization was used standard bolt diameters in inches.

Composite will be changed as well, work describes some cases, namely carbon fiber 90,45,0 degrees of reinforcing.

1. Carbon fiber with 90 degrees of reinforcing

$t_1 = t_2 = 0,148$ in = const

d_i – variable

C_i – fastener flexibility Tate`s method

	1	2	3	4	5	6
Ci (1/in psi)	8.3E-06	5.5E-06	4.1E-06	4.1E-06	5.5E-06	8.3E-06
d (in)	0.125	0.164	0.25	0.25	0.164	0.125
tp (in)	0.148	0.148	0.148	0.148	0.148	0.148
ts (in)	0.148	0.148	0.148	0.148	0.148	0.148
P(lb)	174	170	168	165	161	162

Table 15 Input data

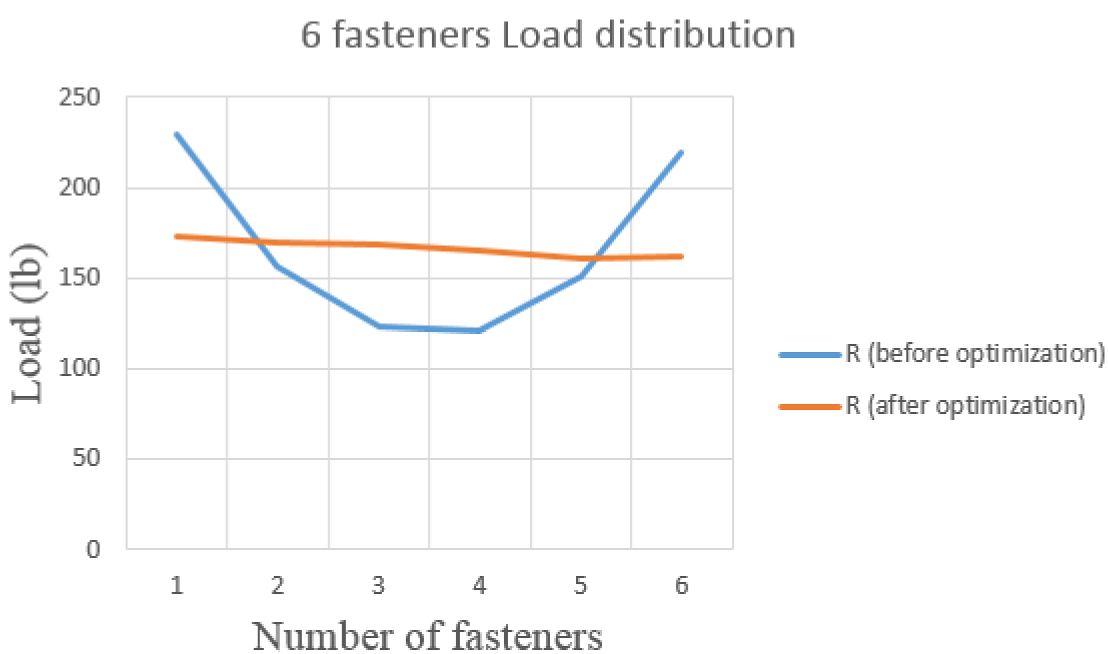

Figure 33 Result of first optimization

At first optimization changing bolt diameters, our distribution isn\`t perfect but it\`s acceptable to design, the reason for unevenly (imperfect) distribution is standard classification of diameters.

2. Carbon fiber with 90 degrees of reinforcing

$t_1 \neq t_2$; t_2 – variable

$d_i = 0.25$ – const

C_i – fastener flexibility Tate\`s method

This work presents only few variants of design the single shear joint with evenly fastener load distribution.

d(in)	0.25	0.25	0.25	0.25	0.25	0.25
Ci (1/in psi)	6.1E-06	4.7E-06	4.2E-06	4.2E-06	4.3E-06	8.0E-06
tp (in)	0.148	0.148	0.148	0.148	0.148	0.148
ts (in)	0.046	0.085	0.13	0.24	0.11	0.03
P (lb)	167	167	163	165	167	169

Table 16 Input for second optimization

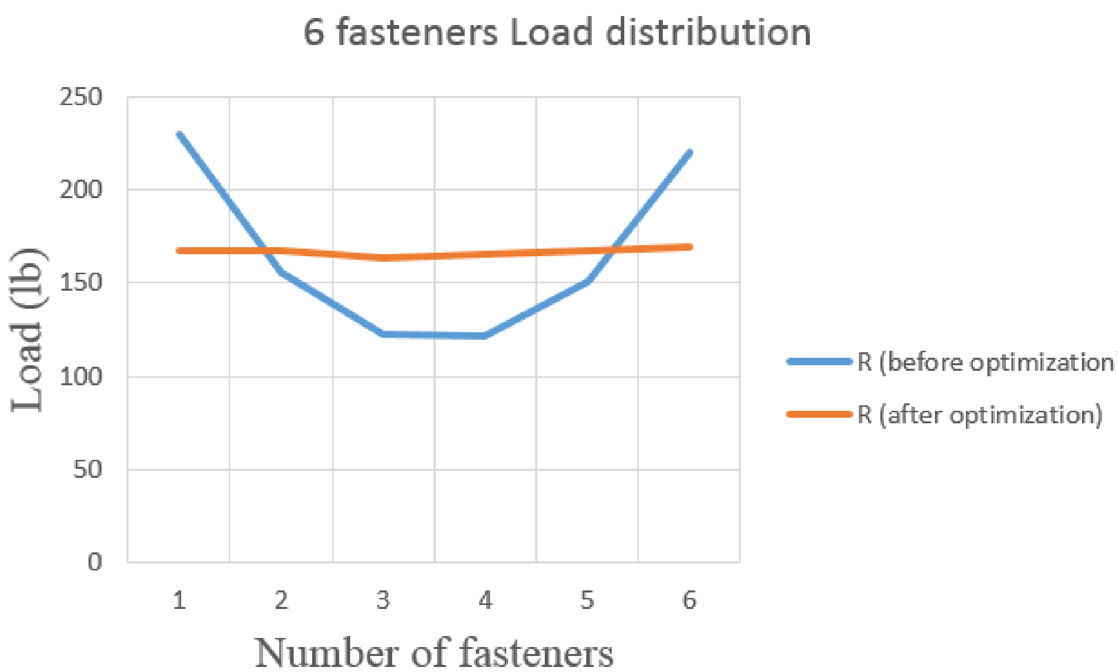

Figure 34 Result of second optimization

As we can see from Table 16 distribution more evenly almost perfect, but this optimization has one big disadvantage, namely the thickness near first and last fastener is little up to 0.03 in. This is hard to design and exploitation. So we can figure this problem out by combining two variants between each other.

Ci (1/in psi)	9.1E-06	5.9E-06	4.1E-06	4.1E-06	4.9E-06	7.5E-06
d (in)	0.125	0.164	0.25	0.25	0.1875	0.125
tp (in)	0.148	0.148	0.148	0.148	0.148	0.148
ts (in)	0.167	0.178	0.14	0.175	0.15	0.125
P (lb)	166.04	167.32	167.05	166.78	166.54	166.27

Table 17 Input for final optimization

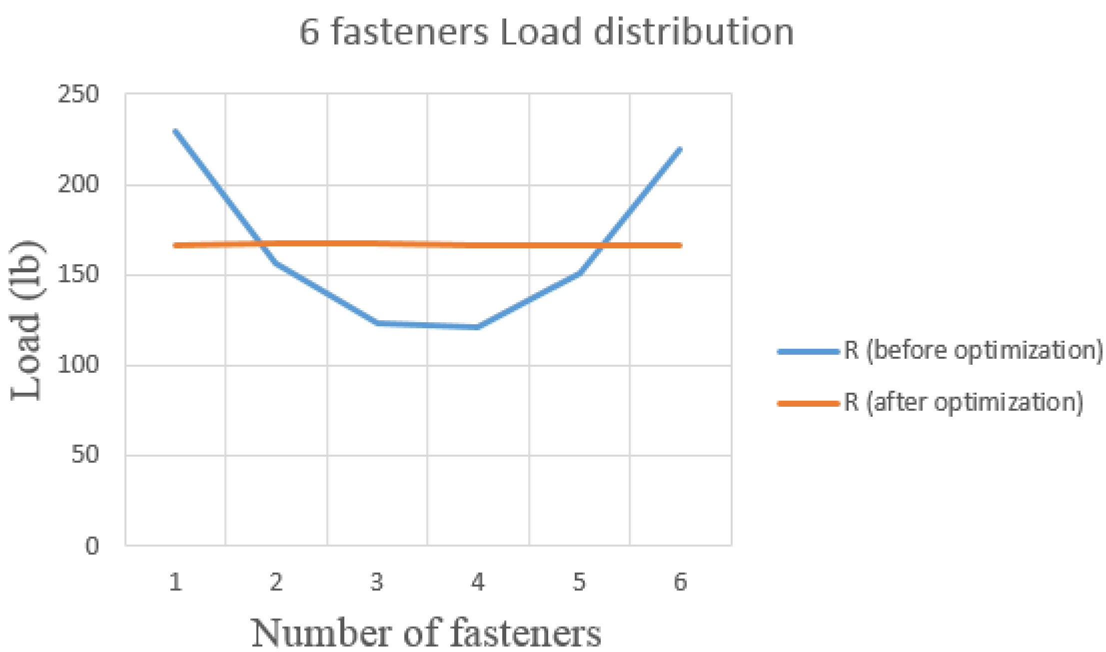

Figure 35 Result of final optimization for 6 fasteners

Finally we get the perfect result, the load distribution is evenly. Combination of changing thickness and bolt diameter gives us perfect result. Then this method of combination will apply to other cases, for load distribution between 2,3,4,5 fasteners.

	1	2	3	4	5
Ci (1/in psi)	7.5E-06	5.3E-06	4.8E-06	5.5E-06	7.6E-06
d (in)	0.125	0.164	0.19	0.164	0.125
tp (in)	0.148	0.148	0.148	0.148	0.148
ts (in)	0.125	0.12	0.14	0.14	0.128
P (lb)	200	200	200	200	200

Table 18 Input data for 5 fasteners

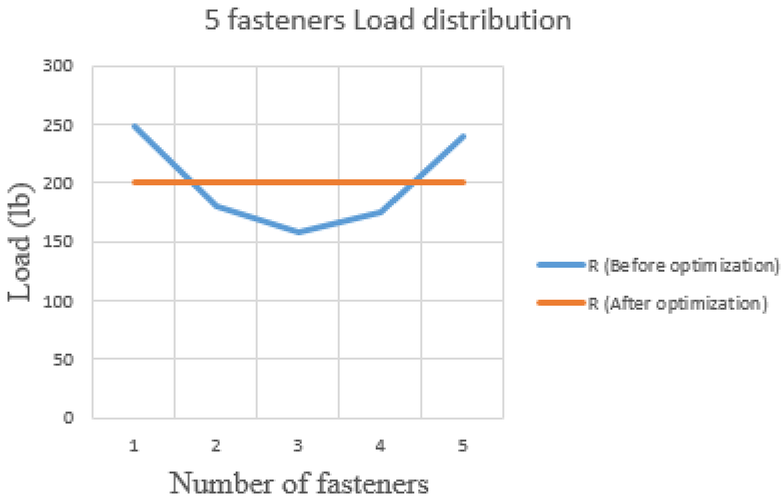

Figure 36 Optimization for 5 fasteners

	1	2	3	4
Ci (1/in psi)	5.7E-06	4.1E-06	4.1E-06	5.5E-06
d (in)	0.164	0.25	0.25	0.164
tp (in)	0.148	0.148	0.148	0.148
ts (in)	0.164	0.137	0.144	0.14
P (lb)	250	250	250	250

Table 19 Input data for 4 fasteners

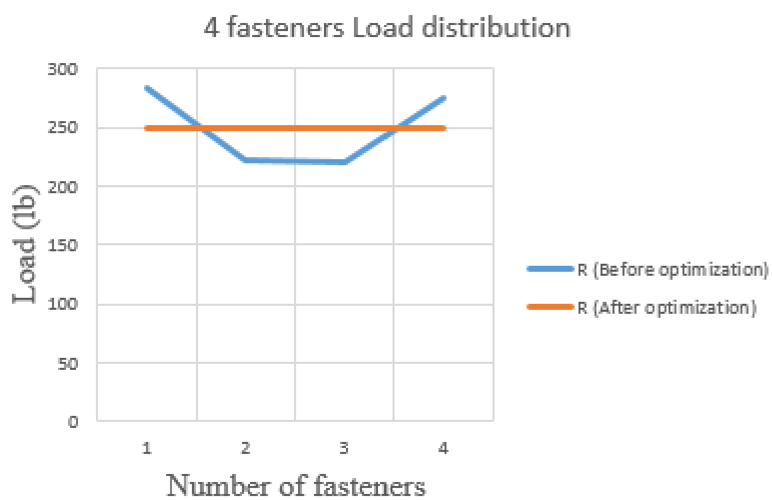

Figure 37 Optimization for 4 fasteners

	1	2	3
Ci (1/in psi)	4,8E-06	4,1E-06	4,8E-06
d (in)	0,19	0,25	0,19
tp (in)	0,148	0,148	0,148
ts (in)	0,123	0,142	0,12
P (lb)	333	333	333

Table 20 Input data for 3 fasteners

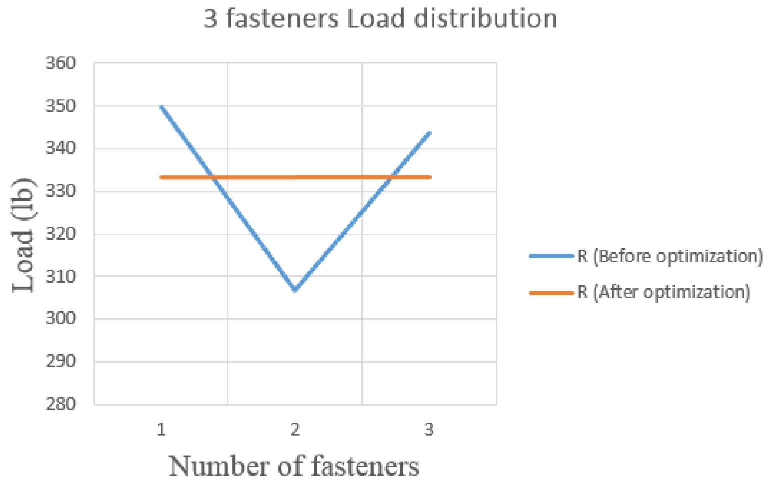

Figure 38 Optimization for 3 fasteners

	1	2
Ci (1/in psi)	4,1E-06	4,1E-06
d (in)	0,25	0,25
tp (in)	0,148	0,148
ts (in)	0,144	0,165
P (lb)	500	500

Table 21 Input data for 2 fasteners

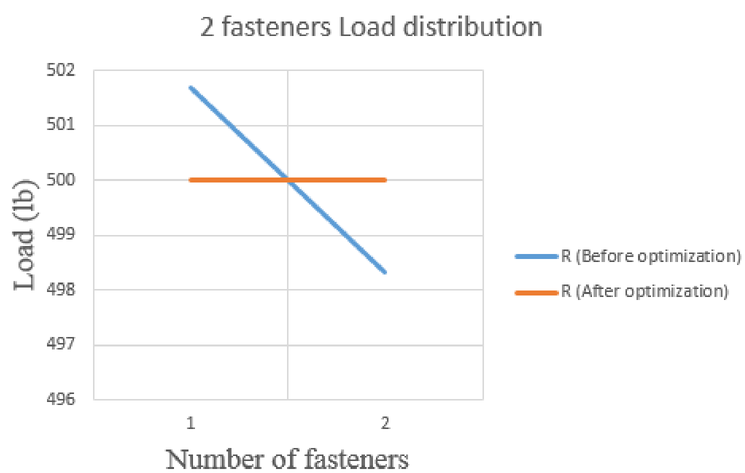

Figure 39 Optimization for 2 fasteners

4. Startup project

4.1. Description of the project idea

The section provides a marketing analysis of the startup project, identifies the opportunities and feasibility of its introduction into the market.

Project Summary	Directions of application	Benefits for the user
Determination of fastener flexibility	Aircraft design, to calculate high loaded joint	1) Simple interface
		2) Determination and optimization are quick and correct

Table 22 Description of the startup project

The new method of determination fastener flexibility investigates the work of metal-composite joints, with the reinforcement of the composite layers 0, ± 15, ± 30, ± 45, ± 60, ± 75, 90 degrees, respectively and helps to do it quick and correct

4.2. Technology audit

It is possible to realize the idea of the project through field tests and statistical analysis. In the Table 23 the analysis of potential technical and economic advantages of this idea in comparison with the competitor # 1 (foreign colleagues in the field of aircraft and machinebuilding).

№	Technical and economic characteristics of the idea	W	N	S
1.	Cash	Competitor №1	—	My project
2.	Method of assessment	—	Competitor №1	My project
3.	Complexity of calculation	—	—	—

Table 23 Determination of strong, weak and neutral characteristics of the project idea

№	The idea of the project	Technology of its implementation	The presence of technology	Technology availability
1.	Determination properties of metal-composite joint	Simple interface	+	+
		Quick access in different devices		
The selected technology can be implemented				

Table 24 Technological feasibility of the project idea

According to the indicators of the state of the market, we can conclude that this project is profitable.

4.3. Analysis of market opportunities for launching a startup project

Determining the market opportunities that can be used in the market implementation of the project, and market threats that may impede the implementation of the project, is quite difficult, given that different methods of solving the task is an element of long-term scientific development of the industry. That is, to evaluate the potential market for a startup project is possible only in the long run, not based on clear numerical characteristics of the market.

Let's analyze the market opportunities for the implementation of our project. To begin with, we will conduct a demand analysis: demand availability, volume and dynamics of market development Table 25

№	Market state indicators	Characteristics
1.	Number of main players, units	2
2.	Total sales, UAH / unit	100
3.	Market dynamics	increase
4.	Sign-in restrictions	Absent
5.	Specific requirements for standardization and certification	available
6.	Average rate of return in the industry,%	100%

Table 25 Preliminary description of a potential startup project market

According to the indicators of the state of the market, we can conclude that this project is profitable.

Identify potential customer groups.

Potential customer groups can be roughly divided into primary and secondary customers. The primary group is the district and regional aircraft. In the future, we will identify potential customer groups Table 26

№	The need that shapes the market	Target audience	Differences in behavior of different potential target customers	Consumer requirements for the product
1.	Unusual reinforcement for composite	Boeing subsidiaries	Finances	Speed of the determination and simplicity

Table 26 Characteristics of potential clients of a startup project

Given the competitive situation, there is an opportunity to work in this market. To be competitive in the market, a project must have characteristics such as the speed of calculation and the availability of software.

Based on the analysis of competition conducted, and taking into account the characteristics of the idea of the project, consumer requirements for the table and factors of the marketing environment, determine and justify the list of factors of competitiveness. The analysis is formalized in Table 27

№	Competitiveness factor	Rationale (citing factors that make the comparison of competing projects meaningful)
1	less need for costs	No need for repeat operations
2	Test accuracy	Improving results
3	The speed of calculation	Maximum resource depletion

Table 27 Rationale for competitiveness factors

According to the identified factors of competitiveness Table 27 we will analyze the strengths and weaknesses of my startup project Table 28

The final stage of market analysis of project implementation opportunities is the compilation of SWOT analysis (Strength and Weak matrix, Troubles and Opportunities on the basis of selected market threats and opportunities, and strengths and weaknesses Table 28

№	Competitiveness factor	Points 1-20	Competitive rating of products compared to the project "Design of high-load single-piece metal-composite compound of minimum mass"						
			-3	-2	-1	0	1	2	3
1	less need for costs	20				●			
2	Accuracy of calculations	20			●				
3	Using the data obtained	20					●		
4	The accuracy of the calculation in the project	15					●		

Table 28 Comparative analysis of strengths and weaknesses " Design of high-load single-piece metal-composite compound of minimum mass”

The list of market threats and market opportunities is compiled on the basis of an analysis of threat factors and factors of the marketing environment. Market threats and market opportunities are the effects of factors and, by contrast, have not yet been realized in the market and are likely to occur.

Based on the SWOT analysis, market behavior alternatives are developed for launching a startup project to the market and an approximate optimal timing of their market implementation in view of potential competitors' projects that may be launched.

The identified alternatives are analyzed in terms of timing and likelihood of receiving resources Table 29

№ п/п	An alternative to market behavior	The probability of receiving resources	Terms of implementation
1	Public review, review of existing studies (analogues), state approval	high	2 months
2	Publication, validation of the present experiment, state approval	High	10 months

Table 29 Alternatives to market introduction of a startup project

From the above alternatives, we will choose the first one, because obtaining resources is simpler and more likely and the timing of implementation is shorter.

Conclusion

1. The program developed in the process of work is similar to the calculations with existing programs, but:
   - Has a simple interface
   - Haven`t got something secret or private like a “black box”
   - Created in Excel program
   - Can be used for create more complex template in Excel.
2. The fastener flexibility is depends on several components, such as: bolt shear, bolt bearing, plate bearing.
3. An extreme fasteners take a big part of the load on it`s necessary to use plate different thickness or diameter with different size.
4. The optimization process for single shear joint, the winding process is very important from the point of view of the weight of the structure and therefore also of the economic value, because it allows evenly distributing the load on the fasteners.

References

1. Johan Soberberg, A finite element method for calculating load distributions in bolted joint assemblies.
2. Карпов Я.С. Соединение деталей и агрегатов из композиционных материалов / Я.С. Карпов. – Х.: Нац. аерокосм. ун-т “Харьк. авиац. ин-т”, 2006. – 359 с.
3. Rotimi Joseph Oluleke. A thesis submitted to the university of Manchester for the degree of doctor of philosophy in the faculty of engineering and physical science.
4. Michael C.Y. Niu .Composite Airframe structures practical design information and data, 1992. – 662 p.
5. M.B. Tate and S. J. Rosenfeld. Preliminary investigation on loads carried by individual bolts in bolted joints. Technical Report TN-1051, National Advisory Committee for Aeronautics, 1946.
6. L. Jarfall. Shear loaded fastener installations. Report KH R-3360, Saab-Scania, 1983.
7. H. Huth. Experimental determination of fastener flexibilities. Report LBF-Bericht 4980, Fraunhofer-Institut fur Betriebsfestigkeit, Darmstadt, 1983.
8. W. Barrois. Stresses and displacements due to load transfer by fasteners in structural assemblies. Engineering fracture Mechanics, 10(1): 115-176, 1978.
9. ESDU. Flexibility of, and load distribution in, multi-bolt lap joints subjected to in-plane axial loads. Data item, Engineering Science Data Unit, 2001.
10. C. Nordin. Bultflexibilitet for drag-och skjuvbelastade skruvforband I KAP. Report FKHK-1-82.045, Saab-Scania, 1982.
11. NASA Contractor report 3710, Critical joints in large composite aircraft structure, 1983, 44pages.
12. Слицкоухов, Ю.В. Конструкции из дерева и пластмасс / Ю.В. Слицкоухов, В.Д. Буданов. – М.: Стройиздат, 1986. – 545с.
13. Гайдачук, А.В. Математическое моделирование процесса отверждения композитной ремонтной накладки / А.В. Гайдачук, Л.В. Смовзюк, М.А.

Шевцова // Авиацеонно-космическая техника и технология. – 2008. - №6. – с. 11-16.

14. ГОСТ 19804-91. Сваи железобетонные. Технические условия. – Взамен ГОСТ 19804.0-78; введен в действие с 28.11.91. – М.: Государственный стандарт СССР, 1991. – 22 с.
15. Карпов, Я.С. Проектирование деталей и агрегатов из композитов: учебник / Я.С. Карпов. – Х.: Нац. Аэрокосм. Ун-т “Харьк. авиац. ин-т”, 2010. – 768 с.
16. H. Huth. Influence of fastener flexibility on the prediction of load transfer and fatigue life for multiple-row joints. Fatigue in Mechanically Fastened Composite and Metallic Joints, ASTM STP927, pages 221-250, 1986.
17. J. Brandt. Formler for berakning av bultflexibilitet. Preliminar utgava. Report FKH R-3303, Saab-Scania., 1982.